WORKING PAPER

A SIMULATION MODEL OF ENVIRONMENTAL PROCESSES
AND VEGETATION PATTERNS IN BOREAL FORESTS:
TEST CASE FAIRBANKS, ALASKA

Gordon B. Bonan

July 1988
WP-88-63

IIASA
International Institute
for Applied Systems Analysis

A SIMULATION MODEL OF ENVIRONMENTAL PROCESSES
AND VEGETATION PATTERNS IN BOREAL FORESTS:
TEST CASE FAIRBANKS, ALASKA

Gordon B. Bonan

July 1988
WP-88-63

ABOUT THE AUTHOR

Gordon B. Bonan participated in the Young Scientists' Summer Program at IIASA in the summer of 1987, working in the Environmental Monitoring Project. He also worked as a Research Scholar in the Biosphere Project at IIASA in the summer of 1988.

His address is: Department of Environmental Sciences, University of Virginia, Charlottesville, Virginia 22903, USA.

FOREWORD

IIASA's project "Ecologically Sustainable Development of the Biosphere" focuses on biotic (ecological) systems, particularly those long term (sustainable) behaviors which are produced in response to human (developmental) activities, and are detected at global (biospheric) spatial scales. An important approach of the "Biosphere" Project to these goals uses mathematical and gaming simulations to explore the complex natural and sociological ramifications of ecosystem responses. The central Biosphere Project study on global vegetation change is being supported by an emerging study aimed at examining the potential future responses of the world's boreal forests to changes in global climate and atmospheric chemistry. The first step is to incorporate known environment-ecosystem relationships into mathematical models, exemplified by the content of this working paper.

The incorporation into models of environmental processes which control the composition and dynamics of northern boreal forests must begin with the critical features of permafrost distribution and dynamics and their inter-relationships with vegetation cover. The current working paper presents a straight-forward approach to solving this problem, verifying the accuracy of the new model routines with vegetation and soils data and field studies in Alaska, USA. This work provides an essential element in our work to produce a globally-comprehensive mathematical model of boreal forest dynamics, and constitutes a basis for broader studies implemented during the summer of 1988 at IIASA.

Allen M. Solomon, Leader
Project "Ecologically Sustainable
Development of the Biosphere"

v

ACKNOWLEDGEMENTS

ABSTRACT

In this study, a simulation model of environmental processes in upland boreal forests was combined with a gap model of species-specific demographic responses to these processes. Required parameters consisted of easily obtainable climatic, soils, and species parameters. The model successfully reproduced seasonal patterns of solar radiation, soil moisture, and depths of freeze and thaw for different topographies at Fairbanks, Alaska. The model also adequately simulated stand structure and vegetation patterns for boreal forests in the uplands of interior Alaska.

These analyses suggest that this modeling approach is valid for upland boreal forests in interior Alaska and have identified the critical processes and parameters required to understand the ecology of these forests. If validated in other bioclimatic regions, this model may provide a framework for a circumpolar comparison of boreal forests and a mechanistic context for bioclimatic classifications of boreal forest regions.

TABLE OF CONTENTS

A SIMULATION MODEL OF ENVIRONMENTAL PROCESSES AND VEGETATION PATTERNS IN BOREAL FORESTS: TEST CASE FAIRBANKS, ALASKA

Gordon B. Bonan

1. Introduction

Boreal forests are a major repository of the world's terrestrial organic carbon (Bolin 1986), and at these latitudes, there is a strong correlation between the seasonal sinusoidal dynamics of atmospheric carbon dioxide and the seasonal dynamics of the "greenness" (Goward et al. 1985) of the earth (Tucker et al. 1986). The association at higher northern latitudes of dynamics of atmospheric carbon dioxide and the dynamics of an index of the productivity of the vegetation (Tucker et al. 1986) is correlative, but a possible causal relation, with the dynamics of the forests at these latitudes driving the atmospheric carbon concentrations, appears to be consistent with the present-day understanding of ecological processes in these ecosystems (Fung et al. 1987; D'Arrigo et al. 1987). Along with its familiar role in plant photosynthesis, carbon dioxide is a "greenhouse" gas that has an active role in affecting the heat budget of the earth (Budyko 1982). Thus, the possibility that boreal forests may actively participate in the dynamics of atmospheric carbon dioxide is of considerable significance, especially since the climatic response to elevated atmospheric carbon dioxide concentrations seems to be strongly directed to the boreal forests of the world (Bolin 1977; Dickinson 1986; Shugart et al. 1986).

These large-scale forest/environment interactions are a motivation to better understand the environmental processes controlling the structure and function of boreal forest ecosystems. Numerous researchers have examined specific aspects of boreal forests (e.g., Tamm 1950, 1953, 1976; Siren 1955; Lutz 1956; Wright and Heinselman 1973; Larsen 1980; Persson 1980; Karpov 1983; Wein and MacLean 1983; Wein et al. 1983; Van Cleve and Dyrness 1983; Johnson 1985; Van Cleve et al. 1986), but as yet, no one has formulated a unifying model of the boreal forest, a paradigm to link the pattern of forest vegetation with the environmental processes that cause those patterns.

The purpose of this paper is to develop a unifying conceptual model of environmental processes and vegetation patterns in boreal forests. Our current understanding of the ecology of boreal forests indicates that the boreal forest is a mosaic of vegetation types that reflects a combination of environmental factors unique to northern forests (Fig. 1). Climate, solar radiation, soil moisture, the presence or absence of permafrost, the forest floor organic layer, nutrient availability, wildfires, and insect outbreaks interact to contribute to the mosaic pattern of forest types and the wide range in stand productivity characteristic of boreal forests (Bonan and Shugart 1989). In this paper, a simple model that characterizes the birth, growth, and death of individual trees is combined with algorithms that simulate these environmental factors to better understand the processes controlling local and regional vegetation patterns in boreal forests. The validity of this model is tested in the upland boreal forests of interior Alaska.

2. Solar Radiation

The theory of "equivalent slopes" (Lee 1962; Lee and Baumgartner 1966) provides a convenient formula to estimate average monthly solar radiation received on a surface located at a given latitude, slope, and aspect (cf. Buffo et al. 1972; Frank and Lee 1966; Swift 1976), and Brock (1981) reviewed other approaches to calculating solar radiation. However, these methods fail to distinguish direct and diffuse radiation, which is a particularly important distinction at high latitudes (Rosenberg et al. 1983). Consequently, in this model average monthly solar radiation is calculated using the methodology developed by Liu and Jordan (1960, 1962, 1963) and Klein (1977) that decomposes total radiation received on a horizontal surface into its direct and diffuse components and then uses various tilt factors to adjust these horizontal components to components on the surface of interest (Fig 2).

2.1 Solar radiation received outside the atmosphere

Average monthly solar radiation is calculated by first determining the amount of solar radiation received on a horizontal surface outside the earth's atmosphere on the days that are representative of the monthly mean (Klein 1977; Brock 1981). This is a function of latitude, the solar declination, and the sunrise/sunset hour angle. Solar declination, D, on the nth day of the year is approximated by (Klein 1977; Brock 1981):

$$D = 23.45° \ SIN \ [360(284+n)/365]$$

The sun sets and rises on a surface when the solar incidence angle is 90° or when the solar altitude angle is 0°, whichever occurs closer to solar noon (Keith and Kreider 1978). In general, it is not possible to derive a closed-form solution for the sunrise/sunset hour angles because of the complexity of the incidence angle equations. However, on a horizontal surface located at a latitude, L, the altitude angle of the sun at sunrise/sunset is 0°, and the sunrise/sunset hour angle, h_s, is (Keith and Kreider 1978):

$$COS \ h_s = -TAN \ L \ TAN \ D$$

The sun never sets when:

$$TAN \ L \ TAN \ D > 1.0$$

In this case, the sunset/sunrise hour angle is equal to 180° (Keith and Kreider 1978). Likewise, the sun never rises above the horizon when:

$$TAN \ L \ TAN \ D < 1.0$$

In this case, the sunset/sunrise hour angle is equal to 0°.

From these angular quantities, the solar radiation received on a horizontal surface at the top of the atmosphere on the nth day is (Klein 1977):

$$H_0 = 458.37 \ S_0 \ [1+0.033 \ COS \ (360n/365)] \ *$$

$$[COS \ L \ COS \ D \ SIN \ h_s + (h_s/57.296) \ SIN \ L \ SIN \ D)]$$

where:

H_o = undepleted solar radiation (cal-cm^{-2}-day^{-1})

S_o = solar constant (2.0 cal-cm^{-2}-min^{-1})

2.2 Direct and diffuse radiation on a horizontal surface

When solar radiation enters the atmosphere, part of the beam is scattered in all directions by air molecules, water vapor, and dust; part is absorbed, primarily by water vapor, carbon dioxide, and ozone; and the remainder reaches the surface layer. The procedure developed by Liu and Jordan (1960, 1962, 1963) and Klein (1977) attenuates solar radiation for these atmospheric effects and then decomposes total horizontal radiation received at the earth's surface into its direct and diffuse components (Fig. 2).

Linear regressions of monthly data from several meteorological stations located throughout northern North America, Scandinavia, and the Soviet Union were developed to attenuate mean monthly solar radiation for atmospheric effects:

North America ($n=10$, $F=1471$, $p<.0001$, $R^2=.961$)

$H = -7.130 + 0.812 H_o - 0.440 H_o$ (c/10)

Scandinavia ($n=5$, $F=1114$, $P<.0001$, $R^2=.976$)

$H = -7.640 + 0.572 H_o - 0.197 H_o$ (c/10)

Soviet Union ($F=2284$, $p<.001$, $R^2=.980$)

$H = -9.525 + 1.122 H_o - 0.817 H_o$ (c/10)

where:

H = mean monthly solar radiation received at the earth's surface (cal-cm^{-2}-day^{-1})

H_o = mean monthly solar radiation at the top of the earth's atmosphere (cal-cm^{-2}-day^{-1})

c = mean monthly cloudiness (in tenths)

Mean monthly solar radiation at the earth's surface and mean monthly cloudiness were obtained from data in Hare and Hay (1974), Johannessen (1970), and Lydolph (1977). Mean monthly solar radiation at the top of the earth's atmosphere was calculated using the procedure outlined in the preceding section.

In the procedure developed by Liu and Jordan (1960, 1962, 1963), the fraction of the solar radiation received on a horizontal surface at the earth's surface that is diffuse radiation is calculated based on the fraction of solar radiation transmitted through the atmosphere (Kreith and Kreider 1978):

$$K_t = H/H_o$$

and

$$H_d/H = 1.0045 + 0.0435 \ K_t - 3.5227 \ K_t^2 + 2.6313 \ K_t^3$$

where:

H_d = diffuse radiation $(cal-cm^2-day^1)$ received on
a horizontal surface at the earth's surface

If $K_t > 0.75$, $H_d/H = 0.166$ (Keith and Kreider 1978).

2.3 Tilt factors

In Liu and Jordan's (1960, 1962, 1963) method, various tilt factors are
used to adjust horizontal direct and diffuse radiation to that received on
the surface of interest. A tilt factor is merely the ratio of solar
radiation received on a tilted surface to that received on a horizontal
surface. For direct radiation, the instantaneous tilt factor, R_b, is
(Keith and Kreider 1978):

$$R_b = COS \ i \ / \ SIN \ a$$

where:

a = solar altitude angle

i = solar incidence angle

To find the long-term tilt factor, the instantaneous tilt factor must be
integrated over the appropriate time interval with the direct beam com-
ponent used as a weighting factor (Keith and Kreider 1978). Explicit
solutions to tilt factors exist for various south-facing surfaces oriented
due south and east or west of south (Klein 1977). However, for non-south
facing surfaces, iterative or numerical methods must be used to approximate
the appropriate tilt factor. In this case, the direct radiation tilt
factor can be approximated by dividing the daily average of COS (i) by the
daily average of SIN (a) for the period in which the sun is both above the
horizon (a>0°) and in front of the surface (i<90°) for the day of the month
representative of mean monthly solar radiation (Keith and Kreider 1978). In
this model, daily averages of COS (i) and SIN (a) are obtained from hourly
calculations of solar incidence and altitude angles.

For a given solar hour angle, h, where:

$$h = 15° \ (t-12)$$

and t is the time (in hours) from midnight, the solar altitude angle, a,
above the horizon is calculated as (Keith and Kreider 1978):

$$SIN \ a = SIN \ L \ SIN \ D + COS \ L \ COS \ D \ COS \ h$$

The solar incidence angle depends on latitude, solar declination, solar
hour angle, and surface orientation (Keith and Kreider 1978). For horizon-
tal surfaces:

$$COS \ i = SIN \ a$$

For surfaces facing due south with a tilt angle, s:

$$COS \ i = SIN \ (L-s) \ SIN \ D + COS \ (L-s) \ COS \ D \ COS \ h$$

For tilted surfaces facing in directions other than due south:

$$COS \ i = COS \ (a_s - a_w) \ COS \ a \ SIN \ s + SIN \ a \ COS \ s$$

The azimuthal angle of the sun from the south, a_s, is (Keith and Kreider 1978):

$$SIN \ a_s = COS \ D \ SIN \ h \ / \ COS \ a$$

The solar azimuth angle is positive east of south and negative west of south (Keith and Kreider 1978).

The wall azimuth angle, a_w, is merely the aspect of the slope from south and is defined so that the angle is positive east of south and negative west of south (Keith and Kreider 1978).

Diffuse radiation received on a tilted surface is different from that received on a horizontal surface because a tilted surface does not intercept radiation from the entire celestial hemisphere, which is the source of diffuse radiation. If the sky is assumed to be an isotropic source of diffuse radiation, the instantaneous and long-term diffuse radiation tilt factors, R_d, are equal to one another and are related to the radiation view factor from the plane to the visible portion of the hemisphere (Keith and Kreider 1978):

$$R_d = COS^2 \ (s/2)$$

Direct beam and diffuse radiation tilt factors are combined to give R_t, the ratio of total radiation received on a tilted surface to that received on a horizontal surface (Liu and Jordan 1962; Klein 1977):

$$R_t = [1 - H_d/H] \ R_b + H_d/H \ R_d$$

The average monthly solar radiation received on the surface is then:

$$H_t = H \ R_t$$

3. Soil Moisture

3.1 Potential evapotranspiration

There are a wide variety of methods to estimate potential evapotranspiration from plant communities. The best known and most widely used of these are the Penman-Monteith equation and Thornthwaite's method. The Penman-Monteith equation is a combination equation (i.e., considers both energy supply and mass transfer of water vapor from the evaporating surface) derived from the leaf energy balance equation (Rosenberg et al. 1983). It provides a rigorous method of combining the energy balance of a leaf with aerodynamic and mass transfer parameters and gives good estimates of transpiration rates from forests (Rosenberg et al. 1983; Landsberg 1986).

However, the generality of this equation is limited because the canopy resistance term can not be easily parameterized (Rosenberg et al. 1983; Landsberg 1986). Moreover, because it is derived from the energy balance of a leaf, the Penman-Monteith equation ignores fluxes of water vapor to and from the soil (Landsberg 1986).

Thornthwaite (1948) and Thornthwaite and Mather (1955, 1957) estimated potential evapotranspiration from mean air temperature because over long time periods air temperature and evapotranspiration are similar functions of net radiation and therefore are autocorrelated (Rosenberg et al. 1983). However over short time periods, mean air temperature is not a suitable measure of incoming solar radiation, and Thornthwaite's method underestimates potential evapotranspiration during the summer when the solar radiation received at the surface is at its annual maximum (Rosenberg et al. 1983). Furthermore, this method does not capture the effect of solar radiation on local soil moisture patterns. This is particularly important in high-latitude boreal forests where the solar elevation angle is low and the effects of slope and aspect on soil moisture are accentuated (Viereck et al. 1983, 1986).

Monthly potential evapotranspiration can be calculated from incoming solar radiation using a modified form of the Priestley and Taylor (1972) formula:

$$E_p = a \; s/(s+k) \; (R_n - G)$$

where:

E_p = potential evapotranspiration

R_n = net radiant flux density

G = soil heat flux density

a = empirical constant

s = slope of the saturation vapor pressure curve at the mean wet bulb temperature of the air

k = thermodynamic psychrometric constant

By assuming that the soil heat flux is equal to zero when averaged over several days and that the net radiant flux is proportional to solar irradiance (R_s) and air temperature (T_a), the Priestley-Taylor equation can be simplified as (Campbell 1977):

$$E_p = a \; (T_a + b) \; R_s$$

where:

a, b = empirically derived constants

This approach was used by Jensen and Haise (1963) and Jensen (1973) to derive the potential evapotranspiration equation used in this model. For months with mean air temperature above 0° C, mean monthly potential evapotranspiration is calculated as (Jensen and Haise 1963; Jensen 1973):

$$E_p = C_t \ (T_a - T_x) \ R_s$$

where:

E_p = mean monthly potential evapotranspiration (cal-cm^{-2}-day^{-1})

T_a = mean monthly air temperature ($^\circ$C)

R_s = mean monthly solar radiation (cal-cm^{-2}-day^{-1})

C_t and T_x are empirical parameters:

$$C_t = [38 - (2 \ E/305) + 380/(e_2 - e_1)]^{-1}$$

$$T_x = -2.5 - 0.14 \ (e_2 - e_1) - E/550$$

where:

E = site elevation (m)

e_2, e_1 = saturation vapor pressures (mb) at the mean maximum and mean minimum temperatures, respectively, of the warmest month of the year

Saturation vapor pressures, e_s (mb), are calculated from air temperature, T_a ($^\circ$C), using Bosen's (1960) approximation:

$$e_s = 33.8639 \ [(0.00738 \ T_a + 0.8072)^8 - 0.000019 \ |1.8 \ T_a + 48| \\ + 0.001316]$$

This approximation is accurate for air temperatures between -51°C and 54°C (Bosen 1960).

The soil moisture content algorithm is based on the amount of water, cm, in a unit area of soil. Potential evapotranspiration is converted from cal-cm^{-2}-day^{-1} to a monthly total (cm) by dividing by the latent heat of vaporization and multiplying by the number of days in the month.

3.2 Soil moisture content

The soil profile is treated as a one- or two-layered system consisting of a forest floor moss-organic layer, if present, and the underlying mineral soil. For each layer in the soil profile, the monthly soil water content is partitioned between ice and unfrozen water. In the first month of each year, the ice content of each layer is initialized at a volumetric moisture content, m, and the unfrozen water content is set to zero. For each month thereafter, the ice and water contents are adjusted for water released in the seasonal thawing of the soil profile, actual water loss, and drainage (Fig. 3).

For the ith month, the water released during thawing of a soil layer is proportional to the depth of thaw in that layer:

$$W_t = m/100 \ (x_i - x_{i-1})$$

where:

w_t = water released during thawing (cm)

m = volumetric water content of soil layer

x_i = depth of thaw in soil layer in the ith month (cm)

x_{i-1} = depth of thaw in previous month (cm)

The moss-organic layer is assumed to be saturated at the onset of thawing and therefore releases water during thawing in proportion to $m = m_{sat}$ (i.e., the volumetric moisture content at saturation). For the mineral soil, the presence of a shallow permafrost table impedes soil drainage, causing the soil water table to be at or near the surface (Rieger et al. 1963; Dimo 1969; Tyrtikov 1973; Van Cleve and Viereck 1981; Viereck et al. 1986). As the permafrost table becomes deeper, drainage conditions improve and soils are not as moist (Rieger et al. 1963; Kryuchkov 1973). This effect is incorporated into the model using a site specific drainage parameter in which m is a linear function between saturation, m_{sat}, and field capacity, m_{fc}, depending on the maximum depth of seasonal thaw, x, during the previous year:

$$m = 0.01471 \, [m_{sat} \, (100-x) + m_{fc} \, (x-32)]$$

$$m = m_{fc} \text{ if } x > 100 \text{ cm}$$

$$m = m_{sat} \text{ if } x < 32 \text{ cm}$$

The critical value x=32 cm is the average depth to permafrost reported in poorly drained Picea mariana stands underlain by permafrost in the vicinity of Fairbanks, Alaska (Viereck et al. 1983). The critical value x=100 cm is the rooting depth of well drained sites without permafrost (Viereck et al. 1983).

If a soil layer is not at least partially thawed, there is no water available to satisfy evapotranspiration demands, and the actual water loss from that layer is equal to zero. When a soil layer is at least partially thawed, the actual water loss is solved by partitioning the potential water loss between the moss-organic layer and the mineral soil layer and adjusting the potential water loss for the actual water loss.

Monthly potential water loss is calculated as precipitation minus potential evapotranspiration. Measured precipitation is almost always less than the actual value, primarily because of wind losses. For example, precipitation is underestimated by 10-15% in Alaska (Ford and Bedford 1987) and by 7% in Sweden (Jansson and Halldin 1980). Consequently, in this model observed monthly precipitation is increased by 10%.

When the potential water loss is positive, precipitation exceeds potential evapotranspiration, and the soil profile is assumed to wet from the top down. Under this favorable moisture balance, the water in excess of evapotranspiration demands is added to the top soil layer. If the water content of a soil layer exceeds the drainage parameter, m, the excess water, w_x, is assumed to drain off into the next layer.

When the potential water loss is negative, the potential water loss is partitioned between the moss-organic layer and the mineral soil layer depending on the relative root distribution in the two layers. If the relative distribution of roots at depth z, r(z), decreases linearly with

depth such that:

$$r(z) = a + b z \qquad \text{and} \qquad \int_0^{z_r} r(z) \, dz = 1$$

where z_r is the maximum rooting depth, then:

$$a = 2 / z_r$$

$$b = -2 / z_r^2$$

and the relative root distribution between depths z_1 and z_2 is:

$$2z/z_r \; [1-z/(2z_r)] \; \Big|_{z_2}^{z_1}$$

This equation closely matches the relative distribution of roots in the organic layer and mineral soil for several soil types found near Fairbanks, Alaska (Table 1). The potential water loss from a soil layer h cm thick is then:

$$pwl = r(h) \; [\text{precipitation} - E_p]$$

When the potential water loss is negative, the actual water loss depends on the potential water loss and the amount of water in the soil layer (Dunne and Leopold 1978). A negative exponential function can be used to estimate the actual water retained in a soil for a given accumulated potential water loss (Pastor and Post 1984, 1985). This equation can be re-written to give the monthly water loss from a soil layer, awl (cm), for a given monthly potential water loss, pwl (cm):

$$awl = -w \; (1 - e^{b \; |pwl|})$$

$$b = 0.00461 - 1.10559 \; w_m$$

where:

w = amount of water (cm) in soil layer

w_m = amount of water (cm) in soil layer at a volumetric moisture content m

The amount of water that a soil layer can hold at a given volumetric moisture content is obtained by multiplying the depth of thaw in the layer by the appropriate volumetric moisture content.

Thus, in the ith month of thawing, the amount of water, w_i, in a soil layer is:

$$w_i = w_{i-1} + w_t - w_x + awl$$

and the amount of water frozen as ice, ice_i, is:

$$ice_i = ice_{i-1} - w_t$$

When the soil profile begins to freeze in autumn, water is assumed to freeze in proportion to the monthly depth of freeze, and the water and ice contents are adjusted accordingly.

The total volumetric moisture content of a soil layer h cm thick is:

$$m_v = (w + ice) / h * 100$$

and the gravimetric moisture content is:

$$m_g = m_v \ 1000 \ kg\text{-}m^{-3} \ / \ d \ kg\text{-}m^{-3} * 100$$

where d is the bulk density of the soil layer.

4. Soil Thermal Regime

There are two general approaches to modeling the soil thermal regime. First, knowledge of the physical and thermal properties of a soil can be combined with principles of energy transfer and heat flow to formulate highly detailed, physically-based computer models of the soil thermal regime. Such models have been developed for the soil thermal regimes at Barrow, Alaska (Goodwin and Outcalt 1975; Outcalt et al. 1975a, b; Outcalt and Goodwin 1980; Goodwin et al. 1984) and Sweden (Jansson and Halldin 1980). However, the generality of these models is restricted by the detailed soils and meteorological parameters and the small time step required to solve the soil thermal calculations.

The theoretical and computational problems involved in solving the fundamental heat flow equations can be avoided by using empirical models that predict soil temperature from more easily measured surface climatological data. For example, the soil heat flux is often a linear function of net radiation (Idso et al. 1975; DeHeer-Amissah et al. 1981; Rosenberg et al. 1983) and can be predicted in the winter from daily maximum and minimum air temperatures, solar radiation, and snow depth (Cary 1982; Zuzel et al. 1986). Soil temperatures at various depths can easily be predicted from above-ground climatic conditions, especially air temperature (Ouellet 1973; Hasfurther and Burman 1974; Bocock et al. 1977; Toy et al. 1978; MacLean and Ayres 1985) or merely the Julian day of the year (Meikle and Treadway 1979, 1981). Though this approach does not require knowledge of the physical processes regulating soil temperature, it does require large data sets to empirically develop and test the functions.

In this model, the depths of seasonal freezing and thawing in the soil profile are solved on a monthly basis using the Stephan formula for freezing and thawing in a multi-layered soil (Carlson 1952; Jumikis 1966; Lunardini 1981). This avoids the small time steps required by physically-based heat flow models and the large data requirements of empirical models while taking into account the physical and thermal properties of the soil, the soil moisture content, the latent heat of fusion of water, and the duration of freezing or thawing (Jumikis 1966; Lunardini 1981). Like most of the simple theory of heat transfer in soils, the Stefan equation solves the fundamental, one-dimensional heat conduction equation while neglecting convective heat flow from precipitation, snow melt, and surface water, which though usually negligible (de Vries 1975) can be an important factor in soil thawing (Moskvin 1974; Ryden and Kostov 1980; Kingsbury and Moore 1987). Furthermore, the Stefan equation provides an approximate solution to heat conduction under the assumption that sensible heat effects are

negligible. This is true if latent heat is much larger than sensible heat effects or if sensible heat effects are small--a condition that is true for soils with high water contents but which may not be true for dry soils (Lunardini 1981). The Stefan equation is also based on the assumption that temperature gradients in the soil are linear. When these conditions are met, Stefan's equation provides an accurate approximation of depths of freezing and thawing in soils (Carlson 1952; Jumikis 1966; Lunardini 1981). When they are not met, the equation will yield depths of freeze that are too large (Lunardini 1981).

4.1 Depth of seasonal freeze and thaw

The soil profile is treated as a two layered system composed of a forest floor moss-organic layer, if present, and an underlying mineral soil layer. Under the Stefan assumption, the degree-days required to freeze or thaw the ith layer are (Jumikis 1966):

$$N_i = h_i \; L_i /24 \; (R + r_i /2)$$

where:

N_i = number of required degree-days ($^\circ$C-day)

h_i = thickness of the ith layer (m)

L_i = latent heat of fusion of the ith layer (kcal-m^{-3})

r_i = thermal resistance of the layer (m^2-$^\circ$C-hr-kcal^{-1})

R = sum of resistances for the overlying layers

The thermal resistance of the ith layer in the soil profile is (Jumikis 1966):

$$r_i = h_i /k_i$$

where:

k_i = thermal conductivity (kcal-m^{-1}-hr^{-1}-$^\circ$C^{-1})

The latent heat of fusion of the ith layer is (Jumikis 1966):

$$L_i = Q \; (m_i /100) \; d_i$$

where:

Q = latent heat of fusion of water (80 kcal-kg^{-1})

m_i = gravimetric moisture content

d_i = bulk density (kg-m^{-3})

For each layer of the soil profile, the monthly depth of freeze or thaw is calculated by comparing the monthly cumulative climatologically available freezing or thawing degree-days, adjusted for surface conditions, to the actual number of degree-days required to freeze or thaw the soil layer (Fig. 4). If the available degree-days are greater than the required

degree-days, the layer completely freezes or thaws, and the available
degree-days are reduced accordingly. If the available degree-days are less
than the amount needed to freeze or thaw the layer, the depth of freeze/-
thaw is (Jumikis 1966):

$$x_i = 24 \ (N_{ca}-N) \ / \ [L_i \ (R + 1/2 \ x_i \ /k_i \ )]$$

where:

x_i = depth of freeze/thaw in the ith layer (m)

N_{ca} = climatologically available degree-days

N = number of degree-days needed to freeze/thaw the overlying
layers

and the total depth of freeze/thaw is:

$$x_t = X + x_i$$

where X is the thickness of the overlying soil layers.

4.2 Physical properties of soil layers

The thermal conductivity of an organic layer is a linear function of
moisture content (de Vries 1975; Jansson and Halldin 1980). Thus, for a
given moisture content, m, the thermal conductivity can be calculated as:

$$k = [k_s \ (m_d-m) + k_d \ (m-m_s)] \ / \ (m_d-m_s)$$

where:

k_s = thermal conductivity at saturation

k_d = thermal conductivity when dry

m_s = moisture content at saturation

m_d = moisture content when dry

Estimates of unfrozen organic layer thermal conductivities range from
0.54-0.40 kcal-m^{-1}-hr^{-1}-^{o}C^{-1} (saturated) to 0.08-0.04 (dry) (Benninghoff
1952; Brown and Johnston 1964; Jumikis 1966; Jansson and Halldin 1980;
Goodwin et al. 1984). For low bulk density organic matter, the frozen
thermal conductivity is equal to the unfrozen thermal conductivity at low
moisture contents and increases to twice the unfrozen value at high
moisture contents (Lunardini 1981). The bulk density of the moss-organic
layer in Picea mariana forests ranges from 20-80 kg-m^{-3} (Dyrness and Grigal
1979; Viereck et al. 1979; Viereck and Dyrness 1979). Estimates of organic
layer bulk density and thermal conductivities used in this model are given
in Table 2.

The thermal properties of northern mineral soils have been described for
North America (Kersten 1949; Lunardini 1981), Sweden (Tamm 1950), and the
Soviet Union (Chudnovskii 1962; Shul'gin 1965; Dimo 1969). Kersten's (1949)
formulas, which calculate mineral soil thermal conductivities from bulk
density and water content, closely correspond to similar data from the

Soviet Union (Lunardini 1981) and are:

fine-textured soils

$$k_t = [0.9 \log_{10} m - 0.2] \, 10^{(0.01 \, d)}$$

$$k_f = 0.01 \, 10^{(0.022 \, d)} + 0.085 \, m \, 10^{(0.006 \, d)}$$

granular soils

$$k_t = (0.7 \log_{10} m + 0.4) \, 10^{(0.01 \, d)}$$

$$k_f = 0.076 \, 10^{(0.013 \, d)} + 0.032 \, m \, 10^{(0.0146 \, d)}$$

where:

k_t , k_f = unfrozen and frozen thermal conductivities
(BTU-in-ft^{-2}-hr^{-1}-^{o}F^{-1})

m = gravimetric soil moisture content

d = soil bulk density (lb-ft^{-3}) (1 lb-ft^{-3} = 16.02 kg-m^{-3})

These thermal conductivities are converted to metric units by:

$$1 \text{ BTU-in-ft}^{-2}\text{-hr}^{-1}\text{-}^{o}\text{F}^{-1} = 0.124 \text{ kcal-m}^{-1}\text{-hr}^{-1}\text{-}^{o}\text{C}^{-1}$$

Bulk densities of mineral soils in the boreal forests of interior Alaska range from 960-1500 kg-m^{-3} (Viereck 1970; Grigal 1979). Mineral soil physical properties used in this study are given in Table 2. Moisture contents of the well drained soil were taken from (Rieger et al. 1963).

4.3 Surface thawing and freezing degree-days

Estimates of surface temperatures are needed to calculate the amount of heat (^{o}C-day) applied to the soil profile during thawing and freezing. One approach has been to derive the equilibrium surface temperature as the surface temperature that balances the energy budget over a specific period of time (Outcalt 1972; Outcalt et al. 1975a, b; Terjung and O'Rourke 1982; Bristow 1987). However, a more simplified approach uses empirically derived corrections factor to adjust air temperature sums for surface conditions (Carlson 1952; Lunardini 1981).

In this model, the empirical correction factor approach is used to adjust the heat load for surface conditions. Several surface conditions based on the presence of a forest cover were devised to approximately correspond with known surface conditions (Table 3). Observed data indicate, for example, that during thawing the presence of a forest cover reduces temperatures at the surface of the mineral soil by 0.37/0.73 = 51%. Thus, the air temperature correction factor for trees on ground surface temperatures is 1.22*0.51 = 0.62. Likewise, the correction factor for freezing is 0.29/0.25*0.33 = 0.38. These values are used for forests in which available light on the forest floor is less than 50% that found in clearings. This critical light value corresponds to the average canopy coverage found in Picea mariana forests in interior Alaska (Slaughter 1983). Other correction factors in relation to canopy coverage are listed in Table 3, and though they are arbitrary, they take into account the effect of increasing stand

density on the soil thermal regime (Tamm 1950; Shul'gin 1965; Moskvin 1974; Chindyaev 1987) and are the best that can be used given the limited data available.

Air temperatures also need to be corrected for the effect of different slopes and aspects on the surface energy budget and depths of freezing and thawing (Tamm 1950; Shul'gin 1965; Dingman and Koutz 1974; Ryden and Kostov 1980; Rosenberg et al. 1983; Rieger 1983; Viereck et al. 1983). On a regional basis, air temperature is a reasonable index of available energy, but it does not capture differences among components of the landscape (e.g., slope, aspect). However, air temperature can be adjusted for slope and aspect by the ratio of solar radiation received on a surface to that received on a horizontal surface at the same latitude (Riley et al. 1973).

5. Forest Floor Organic Layer

Boreal forests are characterized by a thick accumulation of organic matter on the forest floor (Bonan and Shugart 1989). In this model, forest floor characteristics from _Picea mariana_ and _P. glauca_ forests in the uplands of interior Alaska are used to parameterize a simple algorithm for forest floor buildup.

The accumulation of organic matter on the forest floor is modeled as a first-order, linear differential equation in which annual accumulation is the balance between production and decomposition:

$$dw/dt = P_{max} - a\,w$$

where:

w = biomass ($kg-m^{-2}$)

P_{max} = annual production ($kg-m^{-2}$)

a = annual decomposition rate

The solution to this equation is:

$$w(t) = P_{max}/a\,[1-e^{-at}] + w(0)\,e^{-at}$$

where:

$w(t)$ = biomass at year t

$w(0)$ = initial biomass at t=0

and the maximum forest floor biomass is:

$$\lim_{t \to \infty} w(t) = P_{max}/a$$

Maximum reported moss productivity in interior Alaska is 0.20 $kg-m^{-2}$ (Van Cleve and Viereck 1981), and annual decomposition in _Picea mariana_ stands averages 2% (Van Cleve et al. 1983). This gives a maximum forest floor biomass of 10 $kg-m^{-2}$ for _Picea mariana_ forests, which is the same value reported in the literature (Van Cleve and Viereck 1981; Van Cleve et al.

1983; Viereck et al. 1986).

The forest floor depth can be found by dividing biomass by an appropriate conversion factor. For Picea glauca forests in the uplands of interior Alaska, annual decomposition rates average 6.7% (Van Cleve et al. 1983) and the maximum forest floor depth averages 0.10 m (Van Cleve and Viereck 1981). Thus, the appropriate conversion factor is 30 kg-m^{-3}. This value gives a maximum forest floor thickness of 0.33 m in Picea mariana forests. The maximum reported forest floor thickness in Viereck et al.'s (1983) study of Picea mariana stands is 0.38 m.

The annual decomposition rate is a function of soil temperature and ranges from 2% in cold, wet Picea mariana forests underlain with permafrost to 6.7% in warmer, drier Picea glauca forests without permafrost (Van Cleve et al. 1983). This soil temperature effect has been modelled by Q_{10} equations (Bunnell et al. 1977). A similar equation in which annual decomposition is a function of depth of thaw, x, is:

$$a = 0.024 * 1.642^{(x-0.5)/0.5}$$

This equation was derived with the assumptions that a=2% when x=0.32 m (the average depth to permafrost in Picea mariana forests [Viereck et al. 1983]) and that a=6.7% when x=1.54 m (the average depth of thaw in permafrost-free forests [Table 9]).

Mosses thrive in moist, shady environments (Bonan and Shugart 1989). Monthly moss growth is linearly related to the number of days in the month in which the moss is wet (Busby et al. 1978) or the monthly water deficit (Pitkin 1975). In this model, the percent of the growing season in which water content is below the wilting point is used to limit moss grow in relation to soil moisture conditions. Mosses are not allowed to grow if this value exceeds 10% of the growing season. Moss productivity is reduced by high light levels (Bonan and Shugart 1989). Consequently, mosses are not allowed to grow if available light on the forest floor exceeds 75%. Deciduous leaf litter also inhibits the establishment and growth of mosses (Bonan and Shugart 1989). In stands where the deciduous leaf area is greater than 50% of the total leaf area, no mosses are allowed to become established.

6. Fire Regime

The fire regime in boreal forests is characterized by fire frequency, fire intensity, and depth of burn in the forest floor organic layer (Bonan and Shugart 1989). In this model, the annual probability of a stand burning is an input parameter defined as the inverse of the long-term expected fire frequency.

Fuel load conditions are used to classify wildfires into Van Wagner's (1983) gentle, intense, and lethal fire classes:

(1) gentle fires: fuel load < 30%

These low intensity fires kill surface vegetation, but do not scar trees. To simulate this effect, all trees with a diameter at breast height (dbh) less than 12.7 cm are killed regardless of fire tolerance.

(2) intense fires: 30% < fuel load < 60%

These intense fires kill some trees and scar others. For this fire regime, fire tolerant trees are killed if dbh < 17.4 cm. Trees moderately tolerant of fire are killed if dbh < 25.4 cm. Trees intolerant of fire are killed regardless of size.

(3) lethal fires: fuel load > 60%

Lethal fires kill all trees over a wide area. For this fire regime, all trees die regardless of size and fire tolerance.

Fuel load is modelled as the ratio of accumulated stand biomass to a critical fire intensity parameter (e.g., maximum stand biomass). This ratio quantifies Van Wagner's (1979, 1983) hypothetical relationship between potential fire intensity and stand age.

Depth of burn in the organic layer is a linear function of moisture content before burning (Van Wagner 1972; Dyrness and Norum 1983) and preburn depth (Dyrness and Norum 1983). Consequently, the percent reduction in the forest floor due to fire is modelled as:

$$\% = (m_s - m) / (m_s - m_d) + (0.15 + 1.5 h)$$

where:

m = water content of moss-organic layer

m_s = water content when saturated

m_d = water content when dry

h = thickness of moss-organic layer (m)

This equation is based on the assumption that the forest floor is totally consumed by fire when completely dry and otherwise is reduced as a linear function of moisture content and depth.

7. Spruce Budworm Outbreak

In eastern North America, Picea-Abies forests are periodically subjected to severe spruce budworm outbreaks (Bonan and Shugart 1989). These destructive attacks can result in significant mortality among the species susceptible to attack (MacLean 1980). The even-age structure of some Abies balsamea stands in eastern Canada is thought to reflect recent severe budworm attacks (Baskerville 1975). The probability of a budworm outbreak is a complex function of climate and stand structure (Bonan and Shugart 1989). In this model, the probability of attack is an input parameter defined as the inverse of the long term average frequency between budworm outbreaks.

Mature trees are much more vulnerable to attack and suffer higher mortality than young trees (MacLean 1980). For species very susceptible to budworm attacks, 85% of the trees with dbh > 10 cm and 35% of the trees with dbh < 10 cm are assumed to be attacked. For species that are only moderately attacked, 40% of the trees with dbh > 10 cm and 15% of the trees with dbh < 10 cm are assumed to be attacked. These values correspond with budworm induced mortality data from MacLean (1980). Most mortality occurs within 10 years of the start of an outbreak (MacLean 1980). Consequently, trees

subjected to an attack are given a 1% probability of surviving ten additional years.

8. Nutrient Availability

In the boreal forests of North America, site quality declines over successional time as nutrients are tied up in the rapidly accumulating forest floor organic layer (Bonan and Shugart 1989). This model does not directly address this issue because of the numerous complexities needed to model interactions among moss-organic matter accumulation, soil temperature, and nutrient availability (Bonan and Shugart 1989). Instead relative nutrient availability is considered to be a constant input parameter used to adjust tree growth on sites of different relative nutrient quality.

9. Tree Demography

The forest growth model is of the JABOWA (Botkin et al. 1972a, b) and FORET (Shugart and West 1977; Shugart 1984) class of forest succession models that simulate forest dynamics through the effect of available resources on the birth, growth, and death of individual trees on a small forest plot (1/12 ha). These "gap models" have provided a conceptual framework within which to synthesize ecological phenomena (Shugart 1984), and models of this type have been developed for specific forest stands in Scandinavia (Leemans and Prentice 1987; Kellomaki et al. 1987). The main structure of these models consists of two sets of subroutines that simulate environmental and demographic processes. The environmental subroutines determine physical site conditions (climate, solar radiation, available soil moisture, soil thermal characteristics, depth of the organic layer, fire regime, and insect outbreak). The demographic subroutines calculate tree growth and population dynamics based on these site conditions (Fig. 5).

Gap models are stochastic models of forest succession in which many important environmental and demographic processes are solved randomly (e.g., monthly weather, site conditions, mortality, reproduction). Much of the richness in model behavior is directly related to the introduction of randomness. Consequently, there is no closed form solution to the model. Instead, the dynamics of many individual forest plots (in this case 30) are averaged to give the expected dynamics of an idealized forest stand.

9.1 Growth

Optimal tree growth is calculated using the original JABOWA-FORET individual tree growth equation (Shugart 1984). The assumptions required to derive this equation are outlined in Botkin et al. (1972a, b), Shugart and West (1977), and Shugart (1984). A multiplicative reduction factor is then used to scale optimal diameter increment to the extent that available light, soil moisture, nutrient availability, growing degree-days, and depth of seasonal thaw restrict tree growth. Growth multipliers relating individual tree diameter growth to the degree that available light, soil moisture, and growing season temperature sum are limiting have previously been developed (Botkin et al. 1972a, b; Shugart and West 1977; Shugart 1984). Nutrient availability growth multipliers have been developed by Pastor and Post (1985). These equations were relativized to give the relative growth response of trees on sites with different relative nutrient availabilities.

Available Light Growth Multiplier

shade tolerant$\qquad$$rf = 1.00\ [1.0 - e^{-4.64\ (AL - 0.05)}]$

intermediate$\qquad$$rf = 1.32\ [1.0 - e^{-2.51\ (AL - 0.07)}]$

shade intolerant$\qquad$$rf = 2.15\ [1.0 - e^{-1.23\ (AL - 0.09)}]$

$$AL = e^{-.25\,LA}$$

where:

LA = leaf area $(m^2\,m^{-2})$

Soil Moisture Growth Multiplier

$$rf = [(SMOIST - x)\ /\ SMOIST]^{1/2}$$

if $x > SMOIST$, $rf = 0$

where:

SMOIST = maximum percentage of growing season that the species can tolerate soil moisture below the wilting point

x = percentage of growing season with soil moisture below the wilting point

Growing Degree-days Growth Multiplier

$$rf = 4\ (GDD - GDDmin)\ (GDDmax - GDD)\ /\ (GDDmax - GDDmin)^2$$

where:

GDD = available growing degree-days

GDDmin = minimum growing degree-days in species' range

GDDmax = maximum growing degree-days in species' range

Nutrient Availability Growth Multiplier

nutrient stress tolerant$\qquad$$rf = 0.213 + 1.789\ x - 1.014\ x^2$

intermediate$\qquad$$rf = -0.235 + 2.771\ x - 1.550\ x^2$

nutrient stress intolerant$\qquad$$rf = -0.627 + 3.600\ x - 1.994\ x^2$

where:

x = relative nutrient availability
(scaled from 0-1)

In high latitude boreal forests, an additional growth multiplier is needed
to reduced tree growth due to the effects of permafrost. In interior
Alaska, the above-ground biomass of Picea mariana and Picea glauca stands
underlain by permafrost is a quadratic function of the depth to permafrost
(Fig. 6). These equations can be divided by the respective maximum reported
stand biomasses in interior Alaska (Picea mariana: 100 t-ha⁻¹, P. glauca:
250 t-ha⁻¹ [Van Cleve et al. 1983]) to give the relative stand biomass
response to permafrost. Because tree biomass is approximately a squared
function of diameter, the individual tree response to permafrost is
represented by the square root of the stand level response (Fig. 6). These
equations indicate that optimal Picea glauca tree growth occurs on sites
where the active layer is greater than 1.7 m (Fig. 6). Stoeckeler (1952)
stated that optimal growth for Picea glauca occurs on soils unfrozen to a
depth of at least 1.5-1.8 m. These growth multipliers can be generalized by
assuming that Picea mariana represents permafrost tolerant species and
Picea glauca represents species relatively intolerant of permafrost.

9.2 Mortality

Individual trees are subjected to the same age-dependent and stress
mortality as in the FORET model (Shugart and West 1977; Shugart 1984). All
trees are subjected to age-dependent mortality in which they have a 1%
probability of reaching their maximum age under optimal growth conditions.
Trees with an annual diameter increment less than 1 mm for two consecutive
years are subjected to stress mortality in which they have a 1% probability
of surviving ten consecutive years of slow growth. Fire and spruce budworm
outbreaks are additional agents of mortality.

9.3 Reproduction

The annual reproduction algorithm has been substantially changed from that
of the FORET model, which assumed that all species are equally capable of
reproducing in a given year. This assumption is not valid for boreal
forests where major reproduction events following fire reflect pre-burn
stand composition (Dix and Swan 1971; Carleton and Maycock 1978; Larsen
1980; Heinselman 1981; Johnson 1981). In this model, all species are
potentially capable of reproducing in a given year, but the realized
probability of establishment is conditioned by seed availability and
species-specific site preferences.

For each year of simulation, each species is initially assigned a reproduc-
tion index of one. This index is then decremented for site conditions. As
with the growth algorithm, a multiplicative reduction factor is used to
scale seeding probabilities to the extent that available light, soil
moisture, nutrient availability, growing degree-days, and depth of seasonal
thaw are limiting. In addition, if the amount of light on the forest floor
is less than the minimum threshold value for a species, the reproductive
index is set to zero.

The presence of a thick (5-8 cm) moss-organic layer on the forest floor

inhibits successful regeneration (Viereck 1973), though this response varies among species (Zasada 1971). In this model, negative exponential functions scaled to give probabilities of reproducing of either 0.5, 0.25, or 0.125 when the moss-organic layer is 5 cm thick are used to simulate the species-specific detrimental effect of organic matter on reproduction. If the combined site conditions are less than 10% optimal site conditions, the reproduction index is set to zero.

The reproduction index is then scaled for relative seed availability. If in the previous year a species had no mature trees on the plot, the index is decremented by a factor of 0.25. Several switches are used to scale the reproduction indices in response to seed availability following fire. Species with serotinous cones have enhanced seed dispersal following fires (Rowe and Scotter 1973; Viereck 1973; Rowe 1983). If a species has serotinous cones, seed dispersal is increased by a factor of three following a fire if mature individuals were on the plot prior to the fire. Other species such as Betula papyrifera and Populus tremuloides have enhanced seed dispersal following fire because they disperse many light, winged seeds. For these species the reproduction index is increased by a factor of three when there is a fire. Although these switches are somewhat arbitrary, they do mimic the essential reproductive traits of boreal forest tree species (Fowells 1965; Rowe and Scotter 1973; Viereck 1973; Rowe 1983). Shugart and Noble (1981) used a similar approach to model seed availability following fire in Australian forests.

The reproduction indices are summed for all species and relativized to give the annual probability of reproducing for each species. If a species is chosen for reproduction, seven saplings are planted. Diameters at breast height are assigned stochastically with a mean of 1.27 cm. If available light on the forest floor is greater than 95%, the planting algorithm is repeated until the leaf area index is greater than 0.2 m^2 m^{-2}. Shugart and West (1977) used the same procedure to mimic the increased reproduction that occurs upon the opening of a gap in the forest canopy.

Two types of vegetative reproduction are considered. First, root sprouts are planted deterministically as the number of stumps capable of sprouting times a species-specific sprouting index. Individual trees are capable of root sprouting upon death if their diameter at breast height falls within the lower and upper limits for root sprouting and site conditions are not limiting. Second, if a species can reproduce by layering and if site conditions are favorable, an additional seven saplings are planted.

10. Required Parameters

Required species parameters are listed in Table 4. Maximum age, maximum diameter, and maximum height of a species were taken from Fowells (1965). The growth parameter, G, for each species was calculated from maximum age, diameter, and height using the assumptions of Botkin et al. (1972a, b) and Shugart (1984). Shade tolerance classifications were obtained from Fowells (1965). The percentage of the growing season that a species can tolerate drought was taken from Pastor and Post (1985) or the site preferences of the species (Fowells 1965). The tendency for sprouting and the minimum and maximum diameters at breast height for sprouting were taken from Pastor and Post (1985) or estimated from life-history characteristics (Fowells 1965). Nutrient stress tolerances and the growing degree-day parameters were taken from Pastor and Post (1985). Fire tolerance and reproduction characteristics were obtained from Fowells (1965), Zasada (1971), Rowe and Scotter

(1973), Viereck (1973) and Rowe (1983). The ability to grow on permafrost was estimated from range maps and site preferences (Fowells 1965). Vulnerability to spruce budworm attacks was estimated from MacLean (1980).

Required climatic parameters (Table 5) are listed in Table 6. In gap models, climatic parameters such as mean monthly air temperature and monthly precipitation vary stochastically from year to year (Shugart 1984). Long-term monthly averages and standard deviations are used to draw required mean monthly air temperatures from a normal probability distribution and monthly precipitation from a two parameter gamma distribution (Press et al. 1986).

Required soils parameters (Table 5) were obtained from Rieger et al. (1963), and are listed in Table 7 for well drained, moderately drained, and poorly drained soils. In the boreal forests of interior Alaska and Canada, site quality declines over time as nutrients are tied up in the rapidly accumulating forest floor organic matter (Van Cleve et al. 1983; Van Cleve and Yarie 1986). This buildup of the forest floor layer is also associated with a decline in depth of seasonal soil thawing (Dyrness 1982; Viereck 1982). Consequently, explicit changes in the soil nutrient status (i.e., the relative nutrient availability parameter) over time were considered to be correlated with permafrost phenomena and were therefore neglected.

11. Model Validation: Fairbanks, Alaska

11.1 Environmental site conditions

The environmental algorithms were validated by their ability to reproduce seasonal and topographic patterns of site conditions. The solar radiation algorithm captured the essential seasonal dynamics of solar radiation induced by topography at Fairbanks, Alaska (Fig. 7). The potential evapotranspiration algorithm also reproduced the seasonal dynamics of evapotranspiration for Fairbanks, Alaska (Table 8). Estimates of mean monthly solar radiation required for these calculations were supplied by the solar radiation algorithm.

The depth of thaw algorithm was validated by its ability to reproduce characteristics of the soil thermal regime for forested sites located at various elevations and topographies in the vicinity of Fairbanks, Alaska. Air temperatures were adjusted for elevation by a dry adiabatic lapse rate of $1.0°C$ per 100 m (Rosenberg et al. 1983). Required monthly solar radiation and soil moisture estimates were obtained from the preceding algorithms.

The depth of seasonal thaw algorithm provided good estimates of the soil thermal regime in relation to topography, elevation, and the forest floor thickness (Table 9), though depth of seasonal thaw is not necessarily the same as depth to permafrost (Ryden and Kostov 1980; Lunardini 1981). Shallow seasonal thaw depths occurred in poorly drained upland and floodplain sites with a thick forest floor; deep seasonal thaw depths occurred in well drained, south-facing upland and floodplain soils. Simulated seasonal soil freezing and thawing (Fig. 8) corresponded with observed seasonal patterns (Viereck and Dyrness 1979; Ryden and Kostov 1980; Viereck 1982; Chindyaev 1987; Kingsbury and Moore 1987). The algorithm also reproduced the observed decrease in depth of thaw with increased forest floor organic layer thickness (Dyrness 1982; Viereck 1982) (Fig. 9).

These results indicated the importance of soil moisture for the depth of
thaw. Though topography, elevation, forest floor thickness, and soil
drainage interacted to create the mosaic of permafrost patterns found in
interior Alaska (Table 9), these patterns could not be reproduced without
soil drainage differences. Also, the insulating effect of the forest floor
layer depended on the moisture content of the mineral soil (Fig. 9).

Interaction between soil moisture and depth of thaw was, of course, built
into the model. The soil moisture algorithm was developed so that soil
moisture increased up to saturation as the depth of thaw became shallower,
thus mimicing the effects of permafrost on soil hydrology (Benninghoff
1952; Rieger et al. 1963; Dimo 1969; Kryuchkov 1973; Van Cleve and Viereck
1981; Viereck et al. 1986). However as a soil became wetter, the amount of
energy required to thaw the soil increased. Consequently, the soil
moisture content and depth of thaw in one year depended on the soil
moisture content and depth of thaw in the previous year. In all the
simulation cases, however, stable estimates of soil thawing and soil
moisture were obtained after approximately one to five annual interactions
depending on site conditions.

This interaction between soil moisture and soil thawing is an important
component of the soil thermal regime in permafrost soils. For example, when
a fire removes the forest canopy and consumes part of the forest floor, the
heat load on the mineral soil increases, causing the mineral soil to thaw
to a greater depth (Fig. 10). This, in turn, improves soil drainage,
allowing for an even greater depth of thaw in the following year. Eventual-
ly a new equilibrium between depth of thaw and soil moisture is obtained
and the depth of thaw stabilizes (Fig. 10). This suggests that for a given
heat load onto a soil, there is a stable equilibrium between depth of thaw
and soil moisture content. Moreover, these results are consistent with the
reported annual increase in the active layer thickness after removal of
part of the organic layer (Linell 1973; Viereck and Dyrness 1979; Dyrness
1982; Viereck 1982), suggesting that this phenomena is caused, in part, by
improved drainage conditions as the permafrost table recedes.

11.2 Forest dynamics and vegetation patterns

In the uplands of interior Alaska, the boreal forest is a mosaic of
vegetation types that largely reflects fire history and the presence or
absence of permafrost (Viereck et al. 1983, 1986). Picea mariana grows
primarily on cold, wet, nutrient-poor, north-facing or bottom land sites
underlain by permafrost. Picea glauca and the successional hardwoods
(Betula papyrifera, Populus tremuloides) form more productive stands on
warm, mesic, south-facing and bottom land sites without permafrost.

Stand development following a catastrophic fire was simulated for a well
drained, south slope Picea glauca-hardwood stand located on a terrace at
133 m elevation and a poorly drained, 30% north slope Picea mariana stand
at an elevation of 350 m. Lethal fires were assumed to occur in the initial
year of simulation. Thereafter, no fires occurred on either site. The
regeneration algorithm must be parameterized with seed availability data in
the first year of simulation. On the south slope, mature P. glauca, Betula
papyrifera, and Populus tremuloides trees were assumed to be present
immediately prior to the fire. On the north slope, only Picea mariana was
assumed to have mature individuals present prior to the fire. Additionally,
the model must be parameterized with the depth of the moss-organic layer in
the first year of simulation. The fire was assumed to completely consume

the forest floor organic layer on the south slope and to leave a 10 cm
residual organic layer on the north slope. These values correspond with
observed site conditions following fire (Van Cleve and Viereck 1981).

The simulated forest dynamics of the north slope Picea mariana stand
closely matched observed forest succession patterns. Observed data (Van
Cleve and Viereck 1981) show that following fire the active layer increases
significantly for approximately 30 years before decreasing to pre-burn
depths after about 50 years when the forest canopy closes and moss-organic
matter accumulates on the forest floor. A dense Picea mariana stage occurs
between 51-100 years following fire, followed by a gradual breakup as the
stand matures. Simulated stand biomass peaked at about 80 years, which
corresponded with the observed dense stage (Fig. 11). Stand biomass then
declined over time as the forest grew into a mature stand at about 100
years. The fire was assumed to burn the forest floor to a depth 10 cm.
This, combined with the removal of the forest canopy by the fire, resulted
in a greater heat load onto the soil and a greater depth of seasonal thaw
(Fig. 11). This depth of thaw increased to over one meter by year 20, but
decreased sharply to pre-burn depths by the 40th year as the forest canopy
closed and the moss-organic layer accumulated on the forest floor.

Simulated stand structure and site conditions for the mature Picea mariana
forest were representative of a Picea mariana-permafrost forest site near
Fairbanks, Alaska (Table 10). Observed woody biomass and basal area range
from 23.2 t-ha^{-1} and 7 m^2-ha^{-1} on sites with permafrost to 107.6 t-ha^{-1} and
27 m^2-ha^{-1} on permafrost-free sites (Table 10). Predicted woody biomass and
basal area on a Picea mariana forest with a shallow active layer (0.19 m)
averaged 42.3 t-ha^{-1} and 11.6 m^2-ha^{-1}. In addition, site conditions such as
active layer depth, forest floor thickness, and available light on the
forest floor were within the range of reported values in the uplands of
interior Alaska (Table 10).

For these Picea mariana forests underlain by permafrost, a close correspon-
dence between simulated and observed stand structure required that stress
mortality be neglected. In FORET-derived gap models, individuals with an
annual diameter increment less than 0.1 cm are subjected to age-independent
mortality in which they have a 1% probability of surviving ten consecutive
years of slow growth (Shugart 1984). This assumption is not valid for slow
growing species such as Picea mariana with annual growth rates as low as
0.1-0.2 mm (Rencz and Auclair 1978). Instead, trees were assumed to be
stressed when their diameter increment fell below 10% of optimal growth.

Simulated forest dynamics for the south slope forest also corresponded with
observed data. Observed data (Van Cleve and Viereck 1981) show that
hardwoods initially dominate the site for about 100 years following fire,
with Picea glauca relegated to an understory role. The transition to a
Picea glauca overstory occurs at approximately 100 years, allowing the
gradual accumulation of moss-organic matter on the forest floor, and by
year 200, the transition to a Picea glauca-moss forest is complete.
Following fire, the simulated forest was dominated primarily by Betula
papyrifera with a small component of Populus tremuloides (Fig. 12). This
dense hardwood stand began to break up after approximately 50 years. After
125 years, the forest was dominated by Picea glauca and moss-organic matter
began to accumulate on the forest floor, though scattered hardwoods still
remained. By the 200th year, the transition to a mature Picea glauca-moss
forest was complete.

Simulated stand structure during the hardwood stage was close to observed

data (Table 11). Stand density, woody biomass, and forest floor depth for the mature <u>Picea</u> <u>glauca</u> forest also corresponded with observed data (Table 11). However in the mature <u>Picea</u> <u>glauca</u> stand, the maximum predicted stand basal area and stand biomass estimates were much lower than observed values. Stand basal area in the mature stand averaged 25.7 m²-ha⁻¹ with a range of 19.4-29.0 m²-ha⁻¹. Observed basal area ranges from 30-60 m²-ha⁻¹. Similarly, maximum simulated stand biomass was much less than the observed data. Thus, though the model simulated the "average" <u>Picea</u> <u>glauca</u> stand, it did not simulate the most productive stands.

The model was further tested by its ability to simulate landscape vegetation patterns in the upland boreal forests near Fairbanks, Alaska. The model was initialized with topographic, soils, and forest floor organic layer data for 19 <u>Picea</u> <u>mariana</u>, <u>P.</u> <u>glauca</u>, <u>Betula</u> <u>papyrifera</u>, and <u>Populus</u> <u>tremuloides</u> sites listed in Viereck et al. (1983). Soils parameters for these sites are listed in Table 7. In the first year of simulation, each site was burned by a lethal fire, with fire severity calculated from simulated soil moisture conditions. Thereafter, fires were calculated at random with an annual probability of 0.01 (<u>Picea</u> <u>mariana</u> stands) or 0.0057 (<u>Picea</u> <u>glauca</u>-hardwood stands). Critical fire intensity parameters were set to the maximum reported stand biomasses (<u>Picea</u> <u>mariana</u>: 10 kg-m⁻², <u>Picea</u> <u>glauca</u>-hardwoods: 25 kg-m⁻² [Van Cleve et al. 1983]). Seeds for all four species were available following the initial disturbance. Forest growth was simulated for 500 years to approximate equilibrium conditions (Shugart 1984), at which time each site was classified into a forest type based on species dominance. Cold, wet sites with shallow active layers were dominated exclusively by <u>Picea</u> <u>mariana</u> (Fig. 13). Drier sites with deeper active layers were dominated by a mixture of <u>Picea</u> <u>glauca</u> and hardwoods (Fig. 13). These patterns corresponded closely with the observed forest distributions (Viereck et al. 1983, 1986).

12. Conclusion

In this study, a simulation model of environmental processes in upland boreal forests was combined with a FORET-type gap model of species-specific demographic responses to these processes. This model successfully reproduced seasonal patterns of solar radiation, soil moisture, and depths of freeze and thaw for different topographies at Fairbanks, Alaska. This model also adequately predicted stand structure and vegetation patterns for boreal forests in the uplands of interior Alaska. FORET-type models of forest dynamics have previously been developed for numerous temperate and tropical forests (Shugart 1984). The results of this study indicate that this modeling approach is also valid for boreal forests.

Yet these analyses have also identified several FORET-assumptions that may not be not valid in high-latitude boreal forests. As previously discussed, current implementation of stress mortality in FORET-type models (i.e., annual diameter increment less than 0.1 cm) is not appropriate for slow-growing species. Second, the assumptions that allow a relatively simple attenuation of light through the forest canopy in FORET-type models may not be valid in high-latitude boreal forests. Individual tree growth in these models is scaled by the degree that a tree is shaded by taller trees (Shugart 1984). A computationally efficient means of doing this is to assume that (1) the leaf area of a tree is concentrated at the top of the bole and (2) leaf area is distributed uniformly across the simulated forest plot. The low solar elevation angle at high latitudes clearly invalidates the first assumption, and though recent work has begun to address shading

among high-latitude trees (Leemans and Prentice 1987), current versions of
these models can not account for light attenuation along other than
vertical path lengths through the forest canopy.

The light attenuation problems caused by low sun angles may be offset by
adjusting the spatial scale of the simulated forest plot for the low sun
angle. The second light assumption requires that the size of the simulated
forest plot correspond to the zone of influence, or shadow, cast by a large
canopy dominant tree. In low latitudes, where the sun is high above the
horizon during the growing season, this zone is related to the crown area
of a canopy dominant. In high-latitude forests, where the sun is low on the
horizon, this area is more related to the height of a canopy dominant than
to crown area. Indeed, the 1/12 ha plot size used in these analyses
corresponds not with the crown area of boreal forest canopy dominants, but
rather with the long shadow cast by these trees during the growing season.

These analyses have also identified several environmental processes which
though thought to be important in understanding the ecology of boreal
forests, have not yet been adequately explored. First, nutrient avail-
ability was not explicitly considered in this model. Instead, relative
nutrient availability was treated as a constant input parameter. Though
models of nutrient availability at spatial and temporal scales appropriate
to gap models exist (Aber et al. 1978, 1979; Pastor and Post 1985) and may
help to explain forest dynamics in boreal forests (Pastor et al. 1987), the
linkages among important nutrient cycling processes, the moss and lichen
layers, and the soil thermal regime are complex and quantitative data
needed to model these linkages are lacking (Bonan and Shugart 1989).

Second, in permafrost regions of the boreal forest, the forest floor
organic layer, forest canopy closure, soil moisture, and soil thawing are
intricately intertwined, and the interactions among these processes are
essential to modeling any one process. Though some aspects of these
interactions have been examined in detail (e.g., the effect of the forest
floor on the soil thermal regime [Bonan and Shugart 1989]), for the most
part, these relationships are only qualitatively understood. For example,
reduction of the heat load onto the soil by the forest canopy can maintain
permafrost in an otherwise unstable permafrost region (Bonan and Shugart
1989). Yet quantitative interactions among forest canopy structure and the
soil thermal regime are relatively unexplored. Instead, empirical ap-
proximations must be used to adjust the heat load onto the soil in relation
to canopy coverage (Table 3).

Third, an adequate understanding of the ecology of boreal forests requires
a thorough investigation of the effects of moss and lichen mats on tree
growth and regeneration (Bonan and Shugart 1989). However, though thick
moss and lichen mats are thought to preclude tree regeneration (Bonan and
Shugart 1989), the quantitative effects of moss and lichen mats on germina-
tion, establishment, and tree growth are largely unknown. More importantly,
including moss and lichen in the model results in a mixed life-form growth
model with inherent scaling complications in which the growth of the
various life-forms respond to environmental factors at different spatial
and temporal scales.

Despite these problems, the overall ability of this model to simulate
environmental site conditions and forest vegetation patterns in interior
Alaska suggests that the conceptual hypothesis (Fig. 1) developed by Bonan
and Shugart (1989) provides a useful framework in which to understand the
ecology of upland boreal forests. If this is so, then the major environmen-

tal factors needed to understand the ecology of these forests are climate, solar radiation, soil moisture, permafrost, the forest floor organic layer, nutrient availability, forest fires, and insect outbreaks. Certainly, different factors are important in different bioclimatic regions of the boreal forest. This study has identified the critical processes and parameters required to understand the ecology of upland boreal forests in interior Alaska. If validated in other bioclimatic regions, this model may provide a framework for a circumpolar comparison of boreal forests and a mechanistic context for bioclimatic classifications of boreal forests regions.

REFERENCES

Aber, J.D., D.B. Botkin and J.M. Melillo. 1978. Predicting the effects of different harvesting regimes on forest floor dynamics in northern hardwoods. Canadian Journal of Forest Research 8:306-315.

Aber, J.D., D.B. Botkin and J.M. Melillo. 1979. Predicting the effects of different harvesting regimes on productivity and yield in northern hardwoods. Canadian Journal of Forest Research 9:10-14.

Baskerville, G.L. 1975. Spruce budworm: super silviculturalist. Forestry Chronicle 51:138-140.

Benninghoff, W.S. 1952. Interaction of vegetation and soil frost phenomena. Arctic 5:34-44.

Bocock, K.L., J.N.R. Jeffers, D.K. Lindley, J.K. Adamson and C.A. Gill. 1977. Estimating woodland soil temperature from air temperature and other climatic variables. Agricultural Meteorology 18:351-372.

Bolin, B. 1977. Changes of land biota and their importance to the carbon cycle. Science 196:613-615.

Bolin, B. 1986. How much CO_2 will remain in the atmosphere. Pages 93-155 in B. Bolin, B.R. Doos, J. Jager and R.A. Warrick (editors), The Greenhouse Effect, Climatic Change, and Ecosystems. John Wiley, Chichester. 541 pp.

Bonan, G.B. and H.H. Shugart. 1989. Environmental factors and ecological processes in boreal forests. Annual Review of Ecology and Systematics (in press).

Bosen, J.F. 1960. A formula for approximation of the saturation vapor pressure over water. Monthly Weather Review 88:275-276.

Botkin, D.B., J.F. Janak and J.R. Wallis. 1972a. Some ecological consequences of a computer model of forest growth. Journal of Ecology 60:849-873.

Botkin, D.B., J.F. Janak and J.R. Wallis. 1972b. Rationale, limitations and assumptions of a northeastern forest growth simulator. IBM Journal of Research and Development 16:101-116.

Bristow, K.L. 1987. On solving the surface energy balance equation for surface temperatures. Agricultural and Forest Meteorology 39:49-54.

Brock, T.D. 1981. Calculating solar radiation for ecological studies. Ecological Modelling 14:1-19.

Brown, R.J.E. and G.H. Johnston. 1964. Permafrost and related engineering problems. Endeavour 23:66-72.

Budyko, M.I. 1982. The Earth's Climate: Past and Future. Academic Press, New York. 307 pp.

Buffo, J., L.J. Fritschen and J.L. Murphy. 1972. Direct solar radiation on various slopes from 0 to 60 degrees north latitude. United States Forest Service Research Paper PNW-142. 74 pp.

Bunnell, F.L., D.E.N. Tait, P.W. Flanagan and K. Van Cleve. 1977. Microbial respiration and substrate weight loss. I. A general model of the influences of abiotic variables. Soil Biology and Biochemistry 9:33-40.

Busby, J.R., L.C. Bliss and C.D. Hamilton. 1978. Microclimate control of growth rates and habitats of the boreal mosses, Tomenthypnum nitens and Hylocomium splendens. Ecological Monographs 48:95-110.

Campbell, G.S. 1977. An Introduction to Environmental Biophysics. Springer-Verlag, New York. 159 pp.

Carleton, T.J. and P.F. Maycock. 1978. Dynamics of the boreal forest south of James Bay. Canadian Journal of Botany 56:1157-1173.

Carlson, H. 1952. Calculation of depth of thaw in frozen ground. Pages 192-223 in Frost Action in Soils: A Symposium. United States National Research Council, Highway Research Board.

Cary, J.W. 1982. Amount of soil ice predicted from weather observations. Agricultural Meteorology 27:35-43.

Chindyaev, A.S. 1987. Freezing and thawing of drained peat soils in forests of the middle Urals. Soviet Forest Sciences 1987(1):68-72.

Chudnovskii, A.F. 1962. Heat Transfer in the Soil. Israel Program for Scientific Translations, Jerusalem. 164 pp.

D'Arrigo, R., G.C. Jacoby and I.Y. Fung. 1987. Boreal forests and atmosphere-biosphere exchange of carbon dioxide. Nature 329:321-323.

DeHeer-Amissah, A., U. Hogstrom and A.S. Smedman-Hogstrom. 1981. Calculation of sensible and latent heat fluxes and surface resistance from profile data. Boundary-Layer Meteorology 20:35-45.

Dickinson, R.E. 1986. How will climate change? Pages 207-270 in B. Bolin, B.R. Doos, J. Jager and R.A. Warrick (editors), The Greenhouse Effect, Climatic Change, and Ecosystems. John Wiley, Chichester. 541 pp.

Dimo, V.N. 1969. Physical properties and elements of the heat regime of permafrost meadow-forest soils. Pages 119-191 in Permafrost Soils and their Regime. Indian National Scientific Documentation Center, New Delhi. 191 pp.

Dingman, S.L. and F.R. Koutz. 1974. Relations among vegetation, permafrost, and potential insolation in Central Alaska. Arctic and Alpine Research 6:37-42.

Dix, R.L. and J.M.A. Swan. 1971. The roles of disturbance and succession in upland forest at Candle Lake, Saskatchewan. Canadian Journal of Botany 49:657-676.

Dunne, T. and L.B. Leopold. 1978. Water in Environmental Planning. W. H. Freeman and Company, New York. 818 pp.

Dyrness, C.T. 1982. Control of depth to permafrost and soil temperature by the forest floor in black spruce/feathermoss communities. United States Forest Service Research Note PNW-396. 19 pp.

Dyrness, C.T. and D.F. Grigal. 1979. Vegetation-soils relationships along a spruce forest transect in interior Alaska. Canadian Journal of Botany 57:2644-2656.

Dyrness, C.T. and R.A. Norum. 1983. The effects of experimental fires on black spruce forest floors in interior Alaska. Canadian Journal of Forest Research 13:879-893.

Ford, J. and B.L. Bedford. 1987. The hydrology of Alaskan wetlands, U.S.A.: a review. Arctic and Alpine Research 19:209-229.

Fowells, H.A. 1965. Silvics of Forest Trees of the United States. United States Department of Agriculture, Forest Service Handbook Number 271. Government Printing Office, Washington, D.C. 762 pp.

Frank, E.C. and R. Lee. 1966. Potential solar beam irradiation on slopes: Tables for 30° to 50° latitude. United States Forest Service Research Paper RM-18. 116 pp.

Fung, I.Y., C.J. Tucker and I.C. Prentice. 1987. Application of advanced very high resolution radiometer vegetation index to study atmosphere-biosphere exchange of CO_2. Journal of Geophysical Research 92:2999-3015.

Goodwin, C.W. and S.I. Outcalt. 1975. The development of a computer model of the annual snow-soil thermal regime in Arctic Tundra terrain. Pages 227-229 in Proceedings of the AAAS-AMS conference: Climate of the Arctic. Geophysical Institute, University of Alaska, Fairbanks.

Goodwin, C.W., J. Brown and S.I. Outcalt. 1984. Potential responses of permafrost to climatic warming. Pages 92-105 in J.H. McBeath (editor), The Potential Effects of Carbon Dioxide-Induced Climatic Changes in Alaska. School of Agriculture and Land Resources Management, University of Alaska, Fairbanks. Miscellaneous Publication 83-1. 208 pp.

Goward, S.N., C.J. Tucker and D.G. Dye. 1985. North American vegetation patterns observed with the NOAA-7 advanced very high resolution radiometer. Vegetatio 64:3-14.

Grigal, D.F. 1979. Extractable soil nutrients and permafrost under adjacent forest types in interior Alaska. Northwest Science 53:43-50.

Hare, F.K. and J.E. Hay. 1974. The climate of Canada and Alaska. Pages 49-192 in R.A. Bryson and F.K. Hare (editors), Climates of North America. World Survey of Climatology Volume 11. Elsevier Scientific Publishing Company, New York. 420 pp.

Hasfurther, V.R. and R.D. Burman. 1974. Soil temperature modeling using air temperature as a driving mechanism. Transactions of the American Society of Agricultural Engineers 17:78-81.

Heinselman, M.L. 1981. Fire and succession in the conifer forests of Northern North America. Pages 374-405 in D.C. West, H.H. Shugart and D.B. Botkin (editors), Forest Succession. Springer-Verlag, New York. 517 pp.

Idso, S.B., J.K. Aase and R.D. Jackson. 1975. Net radiation-soil heat flux relations as influenced by soil water content variations. Boundary-Layer Meteorology 9:113-122.

Jansson, P-E. and S. Halldin. 1980. Soil water and heat model: technical description. Swedish Coniferous Forest Project, Swedish University of Agricultural Sciences, Uppsala. Technical Report Number 26. 81 pp.

Jensen, M.E. 1973. Consumptive Use of Water and Irrigation Water Requirements. American Society of Civil Engineers, New York. 215 pp.

Jensen, M.E. and H.R. Haise. 1963. Estimating evapotranspiration from solar radiation. Journal of Irrigation and Drainage Division, American Society of Civil Engineers 89:15-41.

Johannessen, T.W. 1970. The climate of Scandinavia. Pages 23-79 in C.C. Wallen (editor), Climates of Northern and Western Europe. World Survey of Climatology Volume 5. Elsevier Scientific Publishing Company, New York. 253 pp.

Johnson, E.A. 1981. Vegetation organization and dynamics of lichen woodland communities in the Northwest Territories, Canada. Ecology 62:200-215.

Johnson, E.A. (editor). 1985. Disturbance and community organization in the boreal forest. Canadian Journal of Forest Research 15:197-293.

Jumikis, A.R. 1966. Thermal Soil Mechanics. Rutgers University Press, New Brunswick, New Jersey. 267 pp.

Karpov, V.G. 1983. Regulation Factors of Spruce Forest Ecosystems. Nauka, Leningrad. 317 pp. (in Russian)

Keith, F. and J.F. Kreider. 1978. Principles of Solar Engineering. Hemisphere Publishing Corporation, Washington, D.C. 778 pp.

Kellomaki, S., T. Kolstrom, A. Makela, E. Valtonen and H. Vaisanen. 1987. Natural succession of tree stands and occurrence of dead trees. University of Joensuu, Joensuu, Finland. 34 pp. (in Finnish)

Kersten, M.S. 1949. Thermal Properties of Soils. University of
    Minnesota, Institute of Technology Bulletin No. 28. 225 pp.

Kingsbury, C.M. and T.R. Moore. 1987. The freeze-thaw cycle of a
    subarctic fen, northern Quebec, Canada. Arctic and Alpine
    Research 19:289-295.

Klein, S.A. 1977. Calculation of monthly average insolation on tilted
    surfaces. Solar Energy 19:325-329.

Kryuchkov, V.V. 1973. The effect of permafrost on the northern tree
    line. Pages 136-138 in Permafrost: Proceedings Second
    International Conference (USSR Contribution). National Academy of
    Sciences, Washington, D.C. 866 pp.

Landsberg, J.J. 1986. Physiological Ecology of Forest Production.
    Academic Press, London. 198 pp.

Larsen, J.A. 1980. The Boreal Ecosystem. Academic Press, New York. 500
    pp.

Lee, R. 1962. Theory of "equivalent slope". Monthly Weather Review
    90:165-166.

Lee, R. and A. Baumgartner. 1966. The topography and insolation climate
    of a mountainous forest area. Forest Science 12:258-267.

Leemans, R. and I.C. Prentice. 1987. Description and simulation of
    tree-layer composition and size distributions in a primaeval
    Picea-Pinus forest. Vegetatio 69:147-156.

Linell, K.A. 1973. Long-term effects of vegetative cover on permafrost
    stability in an area of discontinuous permafrost. Pages 688-693
    in Permafrost: Proceedings Second International Conference
    (North American Contribution). National Academy of Sciences,
    Washington, D.C. 783 pp.

Liu, B.Y.H. and R.C. Jordan. 1960. The interrelationship and
    characteristic distribution of direct, diffuse, and total solar
    radiation. Solar Energy 4:1-19.

Liu, B.Y.H. and R.C. Jordan. 1962. Daily insolation on surfaces tilted
    towards the equator. Transactions of the American Society of
    Heating, Refrigerating, and Air Conditioning Engineers
    67:526-541.

Liu, B.Y.H. and R.C. Jordan. 1963. The long-term average performance of
    flat-plate solar engineering collectors. Solar Energy 7:53-74.

Lydolph, P.E. 1977. Climates of the Soviet Union. World Survey of
    Climatology Volume 7. Elsevier Scientific Publishing Company,
    New York. 443 pp.

Lunardini, V.J. 1981. Heat Transfer in Cold Climates. Van Nostrand
    Reinhold Company, New York. 731 pp.

Lutz, H.F. 1956. Ecological effects of forest fires in the interior of Alaska. United States Department of Agriculture Technical Bulletin 1133. 121 pp.

MacLean, D.A. 1980. Vulnerability of fir-spruce stands during uncontrolled spruce budworm outbreaks: a review and discussion. Forestry Chronicle 56:213-221.

MacLean, S.F. and M.P. Ayres. 1985. Estimation of soil temperature from climatic variables at Barrow, Alaska, U.S.A. Arctic and Alpine Research 17:425-432.

Meikle, R.W. and T.R. Treadway. 1979. A mathematical method for estimating soil temperatures. Soil Science 128:226-242.

Meikle, R.W. and T.R. Treadway. 1981. A mathematical method for estimating soil temperatures in Canada. Soil Science 131:320-326.

Moskvin, Yu.P. 1974. Investigations of the thawing of the active soil layer in the permafrost zone. Soviet Hydrology 1974(5):323-328.

National Oceanic and Atmospheric Administration. 1971-1986. Climatic data: annual summary, Alaska. Volumes 57-72. National Climatic Data Center, Asheville, North Carolina.

Ouellet, C.E. 1973. Macroclimatic model for estimating monthly soil temperatures under short-grass cover in Canada. Canadian Journal of Soil Science 53:263-274.

Outcalt, S.I. 1972. The development and application of a simple digital surface-climate simulator. Journal of Applied Meteorology 11:629-636.

Outcalt, S.I. and C. Goodwin. 1980. A climatological model of surface modification effects on the thermal regime of the active layer at Barrow, Alaska. In Proceedings American Society of Mechanical Engineers, Petroleum Division, Energy Technology Conference, New Orleans, Louisiana. ASME Publication 80-Pet-20. 9 pp.

Outcalt, S.I., C. Goodwin, G. Weller and J. Brown. 1975a. Computer simulation of snowmelt and soil thermal regime at Barrow, Alaska. Water Resources Research 11:709-715.

Outcalt, S.I., C. Goodwin, G. Weller and J. Brown. 1975b. A digital computer simulation of the annual snow and soil thermal regimes at Barrow, Alaska. Cold Regions Research and Engineering Laboratory, Hanover, New Hampshire. Report Number 331. 18 pp.

Pastor, J. and W.M. Post. 1984. Calculating Thornthwaite and Mather's actual evapotranspiration using an approximating function. Canadian Journal of Forest Research 14:466-467.

Pastor, J. and W.M. Post. 1985. Development of a linked forest productivity-soil carbon and nitrogen model. ORNL/TM-9519. Oak Ridge National Laboratory, Oak Ridge, Tennessee. 162 pp.

Pastor, J., R.H. Gardner, V.H. Dale and W.M. Post. 1987. Successional changes in nitrogen availability as a potential factor contributing to spruce declines in boreal North America. Canadian Journal of Forest Research 17:1394-1400.

Persson, T. 1980. Structure and Function of Northern Coniferous Forests: An Ecosystem Study. Ecological Bulletin 32. Swedish Natural Science Research Council, Stockholm. 609 pp.

Pitkin, P.H. 1975. Variability and seasonality in the growth of some corticolous pleurocarpous mosses. Journal of Bryology 8:337-356.

Priestley, C.H.B. and R.J. Taylor. 1972. On the assessment of surface heat flux and evaporation using large-scale parameters. Monthly Weather Review 100:81-92.

Press, W.H., B.P. Flannery, S.A. Teukolsky and W.T. Vetterling. 1986. Numerical Recipes. Cambridge University Press, Cambridge. 818 pp.

Rencz, A.N. and A.N.D. Auclair. 1978. Biomass distribution in a subarctic Picea mariana-Cladonia alpestris woodland. Canadian Journal of Forest Research 8:168-176.

Rieger, S. 1983. The Genesis and Classification of Cold Soils. Academic Press, New York. 230 pp.

Rieger, S., J.A. Dement and D. Sanders. 1963. Soil Survey of Fairbanks Area, Alaska. United States Department of Agriculture, Soil Conservation Service. Series 1959, Number 25. Washington, D.C. 41 pp.

Riley, J.P., E.K. Israelsen and K.O. Eggleston. 1973. Some approaches to snowmelt prediction. Pages 956-971 in The Role of Snowmelt and Ice in Hydrology. International Association of Hydrological Sciences. Publication Number 107, Volume 2.

Rosenberg, N.J., B.L. Blad and S.B. Verma. 1983. Microclimate. Wiley and Sons, New York. 495 pp.

Rowe, J.S. 1983. Concepts of fire effects on plant individuals and species. Pages 135-154 in R.W. Wein and D.A. MacLean (editors), The Role of Fire in Northern Circumpolar Ecosystems. Wiley and Sons, New York. 322 pp.

Rowe, J.S. and G.W. Scotter. 1973. Fire in the boreal forest. Quaternary Research 3:444-464.

Ryden, B.E. and L. Kostov. 1980. Thawing and freezing in tundra soils. In M. Sonesson (editor), Ecology of a Subarctic Mire. Ecological Bulletin (Stockholm) 30:251-281.

Shugart, H.H. 1984. A Theory of Forest Dynamics. Springer-Verlag, New York. 278 pp.

Shugart, H.H. and D.C. West. 1977. Development of an Appalachian deciduous forest succession model and its application to the impact of the chestnut blight. Journal of Environmental Management 5:161-179.

Shugart, H.H. and I.R. Noble. 1981. A computer model of succession and fire response of the high-altitude Eucalyptus forest of the Brindabella Range, Australian Capital Territory. Australian Journal of Ecology 6:149-164.

Shugart, H.H., M.Ya. Antonovsky, P.G. Jarvis and A.P. Sandford. 1986. CO_2, climatic change and forest ecosystems. Pages 475-521 in B. Bolin, B.R. Doos, J. Jager and R.A. Warrick (editors), The Greenhouse Effect, Climatic Change, and Ecosystems. John Wiley, Chichester. 541 pp.

Shul'gin, A.M. 1965. The Temperature Regime of Soils. Israel Program for Scientific Translations, Jerusalem. 218 pp.

Siren, G. 1955. The development of spruce forest on raw humus site in northern Finland and its ecology. Acta Forestalia Fennica 62:1-363.

Slaughter, C.W. 1983. Summer shortwave radiation at a subarctic forest site. Canadian Journal of Forest Research 13:740-746.

Slaughter, C.W. and L.A. Viereck. 1986. Climatic characteristics of the taiga in interior Alaska. Pages 9-21 in K. Van Cleve, F.S. Chapin, P.W. Flanagan, L.A. Viereck and C.T. Dyrness (editors), Forest Ecosystems in the Alaskan Taiga. Springer-Verlag, New York. 230 pp.

Stoeckeler, E.G. 1952. Investigation of military construction in arctic and subarctic regions: trees of interior Alaska, their significance as soils and permafrost indicators. United States Army Corps of Engineers, St. Paul District. 25 pp.

Swift, L.W. 1976. Algorithm for solar radiation on mountain slopes. Water Resources Research 12:108-112.

Tamm, O. 1950. Northern Coniferous Forest Soils. Scrivener Press, Oxford. 253 pp.

Tamm, C.O. 1953. Growth, yield and nutrition in carpets of a forest moss (Hylocomium splendens). Meddelanden Fran Statens Skogsforskningsinstitut 43:1-140.

Tamm, C.O. 1976. Man and the Boreal Forest. Ecological Bulletin 21. Swedish Natural Science Research Council, Stockholm. 153 pp.

Terjung, W.H. and P.A. O'Rourke. 1982. The effect of solar altitude on surface temperatures and energy budget components on two contrasting landscapes. Boundary-Layer Meteorology 24:67-76.

Thornthwaite, C.W. 1948. An approach toward a rational classification of climate. Geophysical Review 38:55-94.

Thornthwaite, C.W. and J.R. Mather. 1955. The water balance. Publications in Climatology Volume 8, Number 1. Drexel Institute of Technology, Centerton, New Jersey. 104 pp.

Thornthwaite, C.W. and J.R. Mather. 1957. Instructions and tables for computing potential evapotranspiration and the water balance. Publications in Climatology Volume 10, Number 3. Drexel Institute of Technology, Centerton, New Jersey. 311 pp.

Toy, T.J., A.J. Kuhaida and B.E. Munson. 1978. The prediction of mean monthly soil temperature from mean monthly air temperature. Soil Science 126:181-189.

Tucker, C.J., I.Y. Fung, C.D. Keeling and R.H. Gammon. 1986. Relationship between atmospheric CO_2 variations and a satellite-derived vegetation index. Nature 319:195-199.

Tyrtikov, A.P. 1973. Permafrost and vegetation. Pages 100-104 in Permafrost: Proceedings Second International Conference (USSR Contribution). National Academy of Sciences, Washington, D.C. 866 pp.

Van Cleve, K. and L.A. Viereck. 1981. Forest succession in relation to nutrient cycling in the boreal forest of Alaska. Pages 185-211 in D.C. West, H.H. Shugart and D.B. Botkin (editors), Forest Succession. Springer-Verlag, New York. 517 pp.

Van Cleve, K. and C.T. Dyrness (editors). 1983. The structure and function of a black spruce forest in relation to other fire-affected taiga ecosystems. Canadian Journal of Forest Research 13:695-916.

Van Cleve, K. and J. Yarie. 1986. Interaction of temperature, moisture, and soil chemistry in controlling nutrient cycling and ecosystem development in the taiga of Alaska. Pages 160-189 in K. Van Cleve, F.S. Chapin, P.W. Flanagan, L.A. Viereck and C.T. Dyrness (editors), Forest Ecosystems in the Alaskan Taiga. Springer-Verlag, New York. 230 pp.

Van Cleve, K., L. Oliver, R. Schlentner, L.A. Viereck and C.T. Dyrness. 1983. Productivity and nutrient cycling in taiga forest ecosystems. Canadian Journal of Forest Research 13:747-766.

Van Cleve, K., F.S. Chapin, P.W. Flanagan, L.A. Viereck and C.T. Dyrness. 1986. Forest Ecosystems in the Alaskan Taiga. Springer-Verlag, New York. 230 pp.

Van Wagner, C.E. 1972. Duff consumption by fire in eastern pine stands. Canadian Journal of Forest Research 2:34-39.

Van Wagner, C.E. 1979. Fuel variation in the natural fire-cycled boreal forest. Pages 67-69 in D. Quintilio (editor), Proceedings International Fire Management Workshop. Canadian Forest Service Information Report NOR-X-215.

Van Wagner, C.E. 1983. Fire behavior in northern conifer forests and shrublands. Pages 65-80 in R.W. Wein and D.A. MacLean (editors), The Role of Fire in Northern Circumpolar Ecosystems. Wiley and Sons, New York. 322 pp.

Viereck, L.A. 1970. Forest succession and soil development adjacent to the Chena River in interior Alaska. Arctic and Alpine Research 2:1-26.

Viereck, L.A. 1973. Wildfire in the taiga of Alaska. Quaternary Research 3:465-495.

Viereck, L.A. 1982. Effects of fire and firelines on active layer thickness and soil temperatures in interior Alaska. Pages 123-135 in Proceedings Fourth Canadian Permafrost Conference. National Research Council of Canada, Ottawa.

Viereck, L.A. and C.T. Dyrness. 1979. Ecological effects of the Wickersham Dome fire near Fairbanks, Alaska. United States Forest Service General Technical Report PNW-90. 71 pp.

Viereck, L.A., K. Van Cleve and C.T. Dyrness. 1986. Forest ecosystem distribution in the taiga environment. Pages 22-43 in K. Van Cleve, F.S. Chapin, P.W. Flanagan, L.A. Viereck and C.T. Dyrness (editors), Forest Ecosystems in the Alaskan Taiga. Springer-Verlag, New York. 230 pp.

Viereck, L.A., C.T. Dyrness, K. Van Cleve and M.J. Foote. 1983. Vegetation, soils, and forest productivity in selected forest types in interior Alaska. Canadian Journal of Forest Research 13:703-720.

Viereck, L.A., J. Foote, C.T. Dyrness, K. Van Cleve, D. Kane and R. Seifert. 1979. Preliminary results of experimental fires in the black spruce type of interior Alaska. United States Forest Service Research Note PNW-332. 27 pp.

de Vries, D.A. 1975. Heat transfer in soils. Pages 5-28 in D.A. de Vries and N.H. Afgan (editors), Heat and Mass Transfer in the Biosphere. I. Transfer Processes in Plant Environment. Scripta Book Company, Washington, D.C. 594 pp.

Wein, R.W. and D.A. MacLean. 1983. The Role of Fire in Northern Circumpolar Ecosystems. Wiley and Sons, New York. 322 pp.

Wein, R.W., R.R. Riewe and I.R. Methven. 1983. Resources and Dynamics of the Boreal Zone. Association of Canadian Universities for Northern Studies, Ottawa. 544 pp.

Wright, H.E. and M.L. Heinselman (editors). 1973. The ecological role of fire in natural conifer forests of western and northern North America. Quaternary Research 3:317-513.

Yarie, J. 1983. Forest community classification of the Porcupine River Drainage, interior Alaska, and its application to forest management. United States Forest Service General Technical Report PNW-154. 68 pp.

Zasada, J.C. 1971. Natural regeneration of interior Alaska forests --
seed, seedbed, and vegetative reproduction considerations. Pages
231-246 in C.W. Slaughter, R.J. Barney and G.M. Hansen (editors),
Fire in the Northern Environment -- A Symposium. United States
Department of Agriculture, Forest Service, Portland, Oregon. 275
pp.

Zuzel, J.F., J.L. Pikul and R.N. Greenwalt. 1986. Point probability
distributions of frozen soil. Journal of Climate and Applied
Meteorology 25:1681-1686.

Table 1. Observed and predicted relative distribution of roots in the organic layer and mineral soil for three soil types found near Fairbanks, Alaska (Viereck et al. 1986).

	Site I	Site II	Site III
forest floor	10 cm	25 cm	15 cm
mineral soil	100 cm	25[1] cm	30[1] cm
rooting depth	100[2] cm	50 cm	45 cm
relative root distribution			
forest floor observed	19% 16%	75% 67%	56% 55%
mineral soil observed	81% 84%	25% 33%	44% 45%

[1] depth to permafrost table

[2] maximum rooting depth is assumed to be 100 cm

Table 2. Physical constants for the organic layer and mineral soil.

A: Organic layer

	Saturation	Dry
bulk density $(kg-m^{-3})$	60	60
volumetric moisture content	39 %	4 %
unfrozen thermal conductivity $(kcal-m^{-1}-hr^{-1}-°C^{-1})$	0.50	0.08
frozen thermal conductivity $(kcal-m^{-1}-hr^{-1}-°C^{-1})$	1.00	0.08

B: Mineral soil

	Well Drained	Poorly Drained
volumetric moisture content		
saturation	35 %	53 %
field capacity	20 %	38 %
dry	6 %	6 %
bulk density $(kg-m^{-3})$	1250	1250
maximum depth (cm)	100	100

Table 3. Correction factors to convert air temperature degree-day sums into surface temperature degree-day sums.

A: Observed Correction Factors (Carlson 1952)

Surface Conditions	Degree-day Correction Factors[1]	
	Thawing	Freezing[2]
spruce trees, brush, and moss over peat soil	0.37	0.29
cleared of trees and brush but with moss over peat soil	0.73	0.25
silt loam cleared and stripped of trees and vegetation	1.22	0.33

B: Simulated Correction Factors

Surface Conditions	Degree-day Correction Factors[3]	
	Thawing	Freezing[2]
0.75 < available light < 1.00	0.92	0.36
0.50 < available light < 0.75	0.77	0.37
0.00 < available light < 0.50	0.62	0.38

[1] temperature at surface of mineral soil

[2] snow not removed

[3] temperature at ground surface

Table 4a. Required species parameters.

AGEMAX -   maximum age of species (yrs)

DBHMAX -   maximum diameter at breast height (cm)

HTMAX -   maximum height (m)

G -   intrinsic growth parameter

LITE -   shade tolerance classification
(1: tolerant, 2: intermediate, 3: intolerant)

SMOIST -   the maximum percentage of the growing season that the species can tolerate soil moisture below the wilting point

NSPRT -   the tendency for stump sprouting

SDMIN -   the minimum diameter at breast height for sprouting (cm)

SDMAX -   the maximum diameter at breast height for sprouting (cm)

FTOL -   fire tolerance (1: tolerant, 2: intermediate, 3: intolerant)

NUTR -   nutrient stress tolerance class
(1: tolerant, 2: intermediate, 3: intolerant)

IPFR -   ability to grow on permafrost (1: good, 2: poor)

IMOL -   ability to reproduce on moss-organic layer
(1: tolerant, 2: intermediate, 3: intolerant)

IBW -   vulnerability to spruce budworm outbreaks
(1: high, 2: low, 3: zero)

ALC -   light level at which reproduction is inhibited

GDDmin -   minimum growing degree-days in the species' range

GDDmax -   maximum growing degree-days in the species' range

SWTCH -   reproduction switches [SWTCH(1) is true if the species has serotinous cones. SWTCH(2) is true if the species has copious wind-dispersed seeds. SWTCH(3) is true if the species can reproduce by layering].

Table 4b. Species parameters for boreal forests in the uplands of interior Alaska.

	Picea mariana	Picea glauca	Populus tremuloides	Betula papyrifera
AGEMAX	250	200	150	140
DBHMAX	46	76	91	76
HTMAX	27	34	30	30
G	93.5	147.3	175.6	187.2
LITE	1	1	3	3
SMOIST	0.30	0.30	0.40	0.30
NSPRT	0	0	3	1
SDMIN	-	-	10	10
SDMAX	-	-	91	32
KTOL	3	3	3	3
NUTR	1	3	2	1
IPFR	1	2	2	2
IMOL	1	2	3	2
IBW	2	2	3	3
ALC	0.0	0.0	0.6	0.6
GDDmin	247	280	280	280
GDDmax	1911	1911	2461	2036
SWTCH	TFT	FFF	FTF	FTF

44

Table 5. Required site parameters.

A: Climatic Parameters

---

latitude, longitude, and elevation of climatic station

long-term mean monthly temperatures (°C) and standard deviations

long-term monthly rainfall (cm) and standard deviations

monthly cloudiness (tenths of the sky covered)

mean maximum and minimum daily temperatures for the warmest month of the year

---

B: Site Parameters

---

aspect, percent slope, and elevation of site

volumetric mineral soil moisture contents at saturation, field capacity, and wilting point

relative site quality* (0-1)

relative fire intensity parameter (kg-m^{-2})

probability of fire (yr^{-1})

probability of spruce budworm outbreak* (yr^{-1})

annual moss productivity (kg-m^{-2})

initial depth of forest floor organic layer (m)

---

* not used in Fairbanks, Alaska test of model

Table 6. Climatic parameters for Fairbanks, Alaska: means, standard
deviations (parentheses), and mean minimum/maximum [brackets]. Source: Hare
and Hay (1974), NOAA (1971-1976).

latitude 64.8°N, longitude 147.9°W, elevation 133 m

Month	Temperature (°C)		Precipitation (cm)	Cloudiness (tenths)
J	-23.9 (7.1)		2.3 (0.5)	6.7
F	-19.4 (6.0)		1.3 (0.7)	6.4
M	-12.8 (4.2)		1.0 (0.4)	6.3
A	-1.4 (3.0)		0.6 (0.7)	6.2
M	8.4 (1.1)		1.8 (1.1)	7.0
J	14.7 (1.4)		3.5 (1.8)	7.3
J	15.4 (1.4)	[1,34]	4.7 (1.5)	7.2
A	12.4 (1.6)		5.6 (1.9)	7.7
S	6.4 (1.6)		2.8 (2.2)	7.9
O	-3.2 (2.3)		2.2 (1.2)	8.1
N	-15.6 (4.6)		1.5 (1.0)	7.0
D	-22.1 (4.8)		1.4 (2.1)	7.1

Table 7. Soils parameters, Fairbanks, Alaska.

	Well Drained	Moderately Drained	Poorly Drained
volumetric moisture content			
saturation	35 %	44 %	53 %
field capacity	20	29	38
wilting point	6	6	6
moss productivity (kg-m^{-2})	0.20	0.20	0.20

Table 8. Comparison of observed and predicted potential evapotranspiration regimes for Fairbanks, Alaska.

| Month | OBSERVED[1] | | | PREDICTED |
	Mean	Minimum	Maximum	
June	12.2 cm	8.8 cm	16.0 cm	11.8 cm
July	12.6	8.2	17.1	11.7
August	8.7	6.5	13.3	7.0

[1] National Oceanic and Atmospheric Administration. 1972-1986. Climatic Data: Annual Summary, Alaska. Volumes 58-72. National Climatic Data Center, Asheville, North Carolina.

Table 9. Observed depth to permafrost and predicted depth of seasonal thaw for several sites near Fairbanks, Alaska. Source: Viereck et al. (1983).

					Observed	Predicted
Slope	Aspect	Elevation	Drainage[1]	Forest floor	Permafrost[2] depth	Thaw[3] depth
Uplands						
30%	N	427 m	PD	38 cm	22 cm	22 cm
0	–	167	PD	14	55	59
10	SE	385	PD	23	35	31
0	–	468	MD	12	–	–
0	–	343	MD	19	–	–
15	NW	470	MD	17	–	–
12	S	747	MD	10	–	–
25	S	396	WD	9	–	129
18	SE	229	WD	6	–	154
Floodplain						
0	–	177	PD	25	16	30
0	–	122	PD	19	20	39
0	–	120	WD	18	–	116
0	–	177	WD	5	–	153
0	–	120	WD	15	–	125

[1] Drainage class (see Table 7)
    PD = poorly drained
    MD = moderately drained
    WD = well drained

[2] – = no permafrost

[3] – = depth of thaw exceeded depth to bedrock (50 cm)

Table 10. Simulated and observed stand structure and site conditions for mature upland <u>Picea</u> <u>mariana</u> stands, Fairbanks, Alaska. Numbers in parentheses are ranges.

Simulated Stand Structure		Observed[1]
Age	100 years	-
Density	2386 ha^{-1} (1812-2784)	2200 ha^{-1} (1400-4000)
Basal Area	11.6 m^2-ha[-1] (9.5-12.9)	14 m^2-ha[-1] (7-27)
Woody Biomass	42.3 t-ha[-1] (34.8-47.1)	50.9 t-ha[-1] (23.2-107.6)
Forest Floor Biomass	88.5 t-ha[-1]	- (76.2-92.2)

Simulated Site Conditions		Observed
Depth to Permafrost[2]	0.19 m (0.19-0.25)	- (0.16-none)
Forest Floor Depth[2]	0.30 m	0.21 m (0.12-0.38)
Available Light at Forest Floor[3]	0.45 (0.42-0.52)	0.46 (0.33-0.60)

[1] Van Cleve et al. 1983, Viereck et al. 1986

[2] Viereck et al. 1983

[3] Slaughter 1983

Table 11. Simulated and observed stand structure for upland Betula papyrifera and Picea glauca stands, Fairbanks, Alaska. Numbers in parentheses are ranges.

Betula papyrifera

	Simulated Stand Structure	Observed[1]
Age	50 years	-
Density	1706 ha^{-1} (1140-2208)	2100 ha^{-1}
Basal Area	25.2 m²-ha[-1] (19.9-29.1)	- (30-35)
Woody Biomass	133.2 t-ha[-1] (102.3-152.8)	111.6 t-ha[-1] (91.9-147.1)

Picea glauca

	Simulated Stand Structure	Observed[1]
Age	150 years	-
Density	1002 ha^{-1} (336-2220)	- (550-1000)
Basal Area	25.7 m²-ha[-1] (19.4-29.0)	- (30-60)
Woody Biomass	144.3 t-ha[-1] (104.3-174.7)	174.4 t-ha[-1] (61.5-245.8)
Forest Floor Depth	9 cm (7-10)	10 cm

[1] Van Cleve et al. 1983, Viereck et al. 1986

Figure 1. Hypothesized environmental processes controlling forest structure and vegetation patterns in upland boreal forests. Dashed boxes represent climatic and edaphic input parameters and processes. Arrows indicate interacting processes.

SOLAR RADIATION

EXTRA-TERRESTRIAL RADIATION

solar constant

latitude

declination

radius vector

ABSORPTION
(cloud cover)

REFLECTION
(cloud cover)

ATMOSPHERE

- BOUNDARY LAYER - - - - - - - - - -

DIRECT RADIATION
(slope, aspect)

DIFFUSE RADIATION
(slope, aspect)

Figure 2. Schematic representation of solar radiation algorithm.

SOIL MOISTURE

EVAPOTRANSPIRATION

PRECIPITATION

FOREST FLOOR ORGANIC LAYER

DRAINAGE

MINERAL SOIL

WATER RELEASED
IN
SOIL THAWING

DRAINAGE
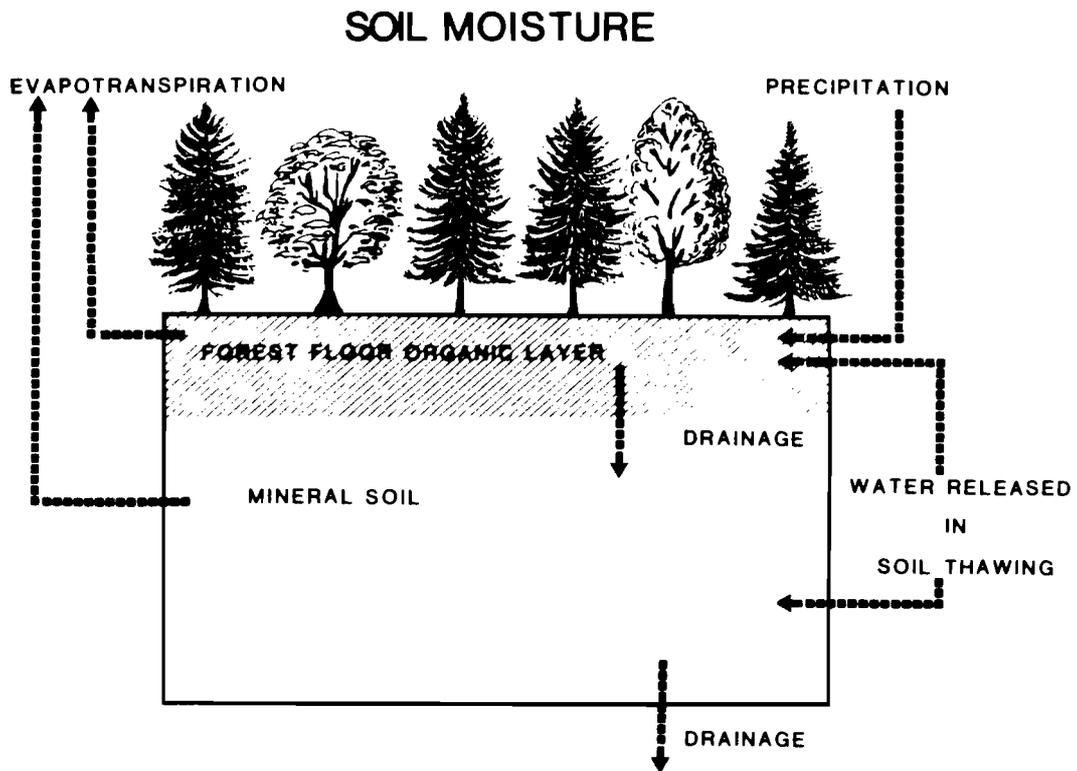
Figure 3. Schematic representation soil moisture algorithm.

DEPTH OF SEASONAL THAW
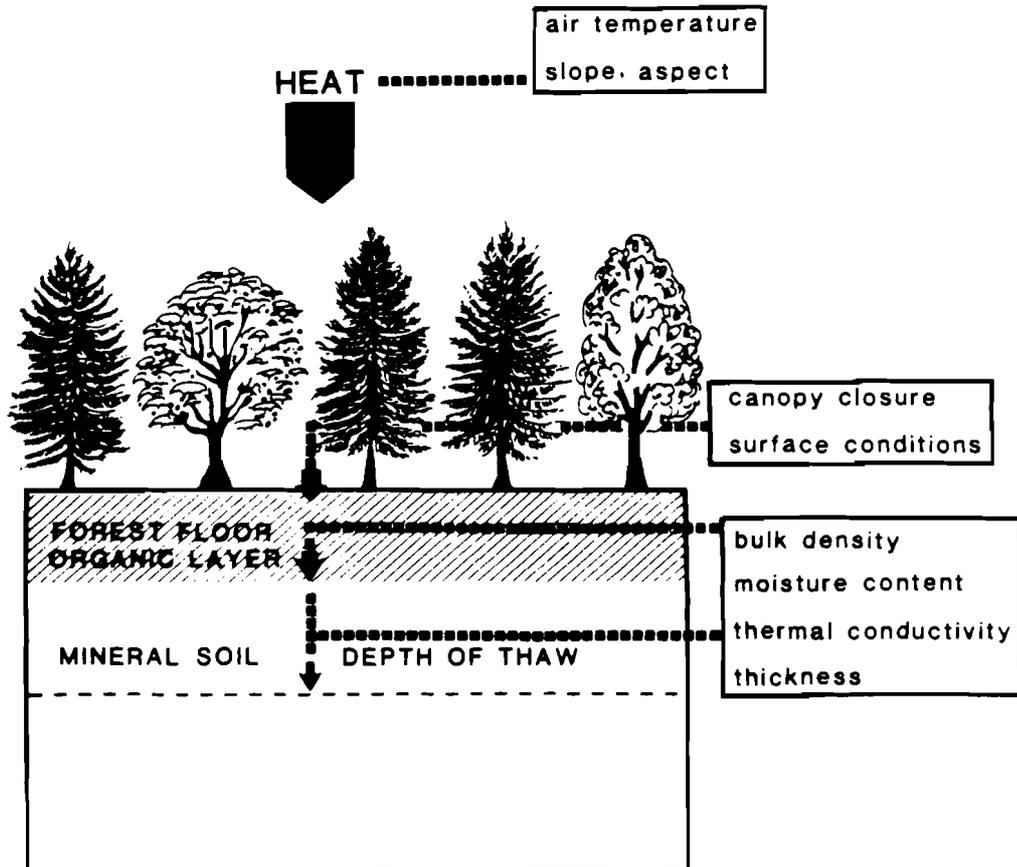
Figure 4. Schematic representation of soil freezing and thawing algorithm.

MORTALITY

ENVIRONMENTAL
CONSTRAINTS

stress
fire
insects

POTENTIAL
LONGEVITY

age

GROWTH

ENVIRONMENTAL
CONSTRAINTS

available light
soil moisture
site quality
growing degree-days
depth of seasonal thaw

POTENTIAL
GROWTH

diameter, age, height

REGENERATION

ENVIRONMENTAL
CONSTRAINTS

available light
soil moisture
site quality
growing degree-days
depth of seasonal thaw
seed bed conditions

POTENTIAL
REPRODUCTION

seed availability
sprouting, layering

Figure 5. Schematic representation of forest growth model.

PORCUPINE PLATEAU AND YUKON FLATS, ALASKA
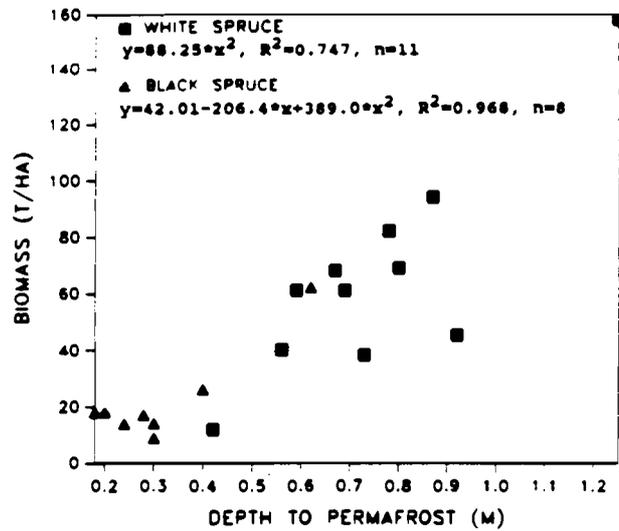
ACTIVE LAYER GROWTH MULTIPLIER
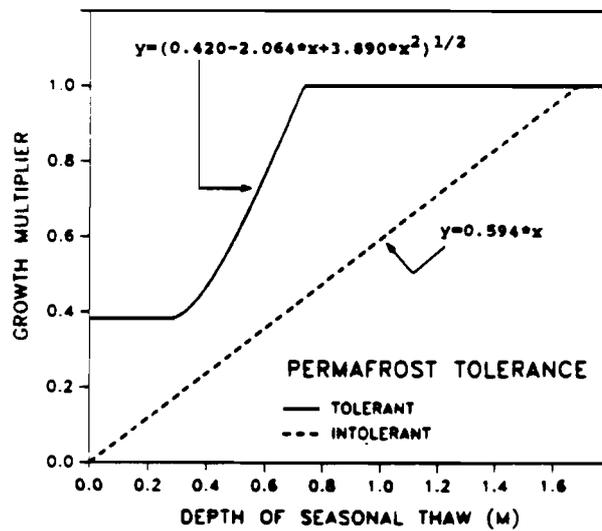
Figure 6. A: Stand biomass in relation to depth to permafrost for black spruce (Picea mariana) and white spruce (Picea glauca) stands in the Porcupine Plateau-Yukon Flats physiographic region of interior Alaska (Yarie 1983). B: Growth multipliers in relation to depth to permafrost.

FAIRBANKS, ALASKA
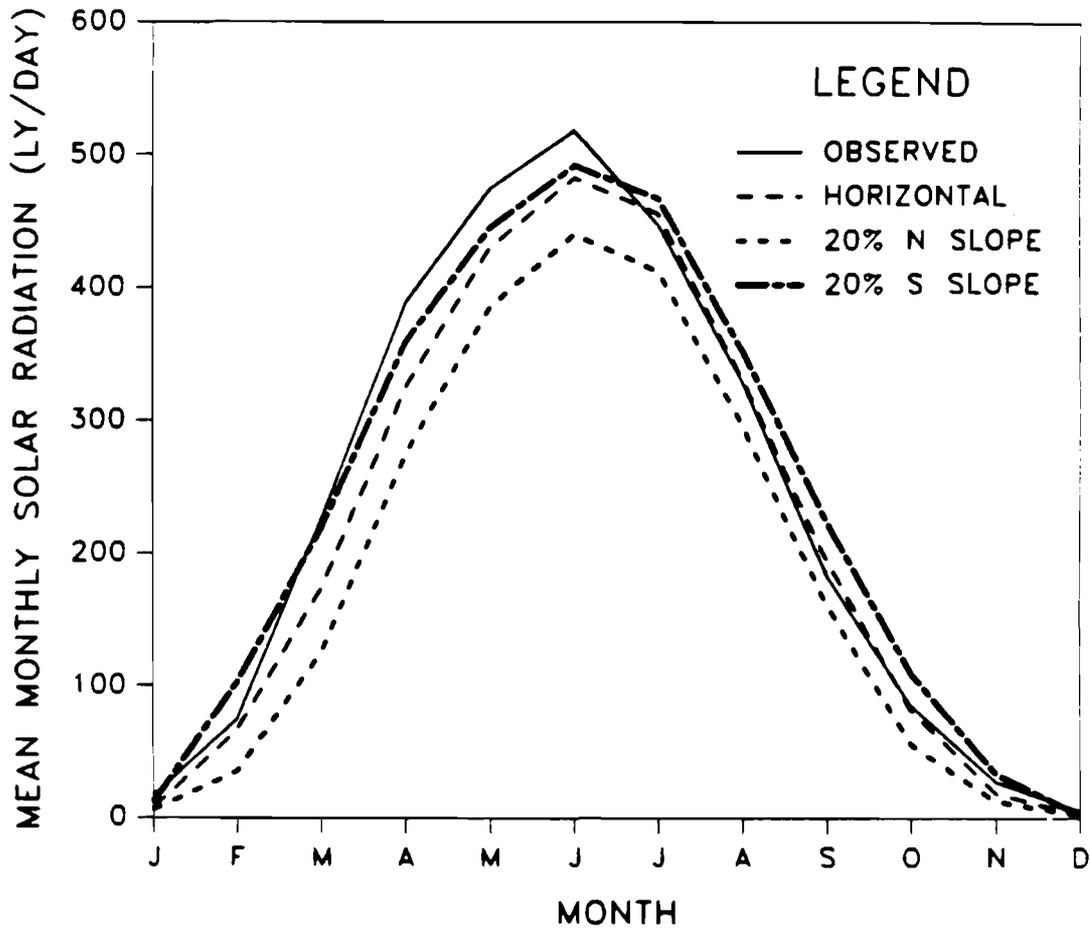
Figure 7. Predicted mean monthly solar radiation received on a horizontal surface, a 20% north slope, and a 20% south slope at Fairbanks, Alaska. Observed data are from Slaughter and Viereck (1986).
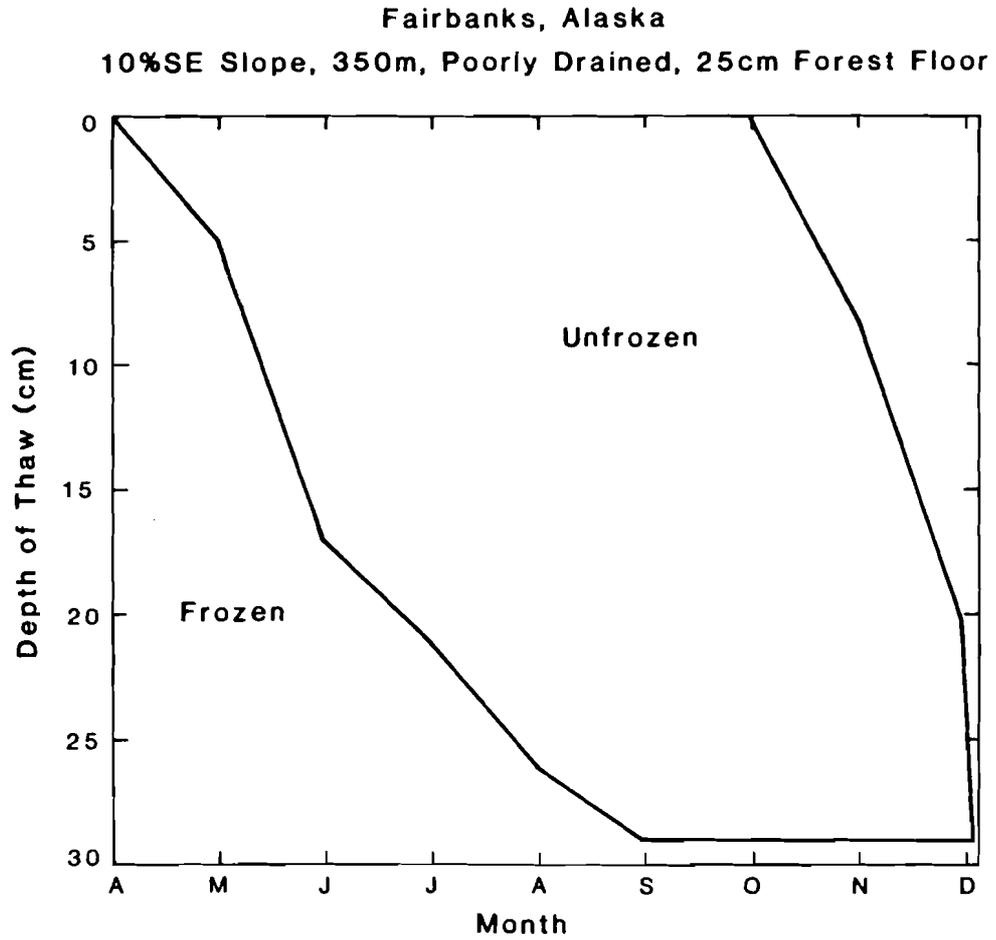
Figure 8. Predicted seasonal soil freezing and thawing, Fairbanks, Alaska.
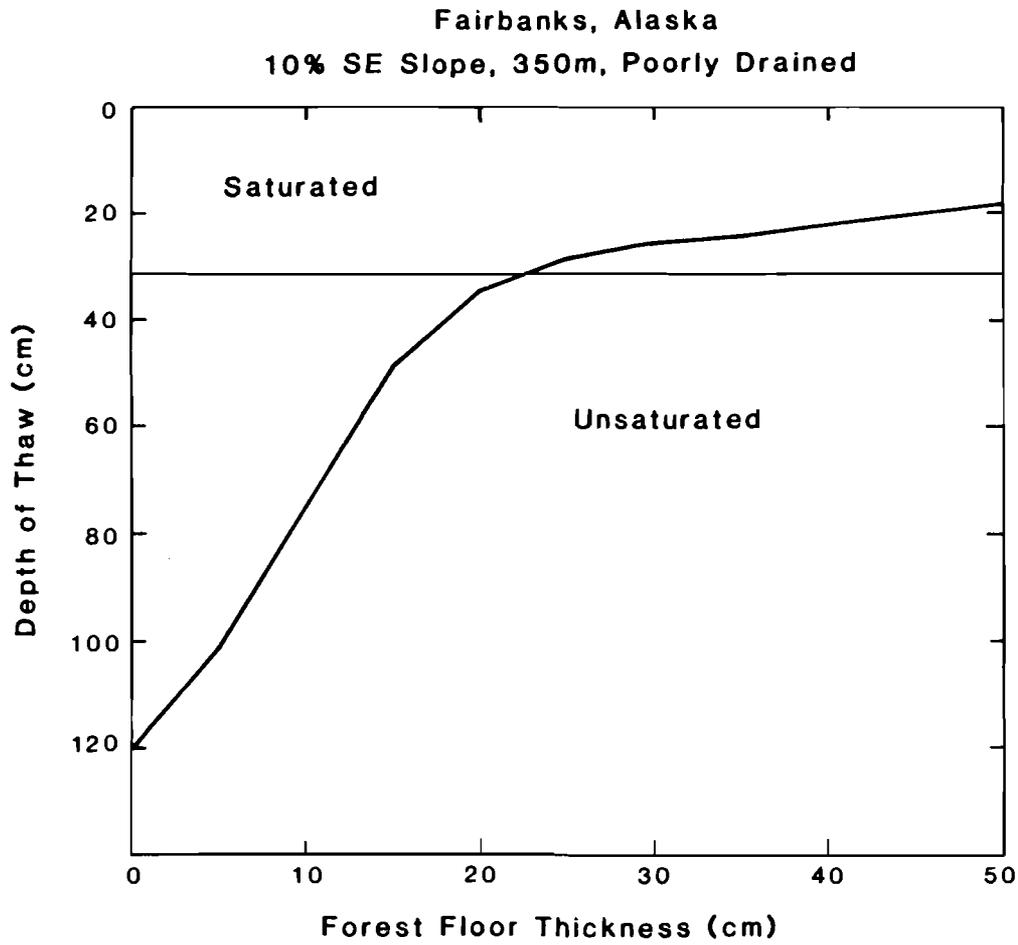
Figure 9. Predicted depth of seasonal thaw in mineral soil at Fairbanks, Alaska, in relation to forest floor thickness.

Fairbanks, Alaska
10% SE Slope, 350m, Poorly Drained
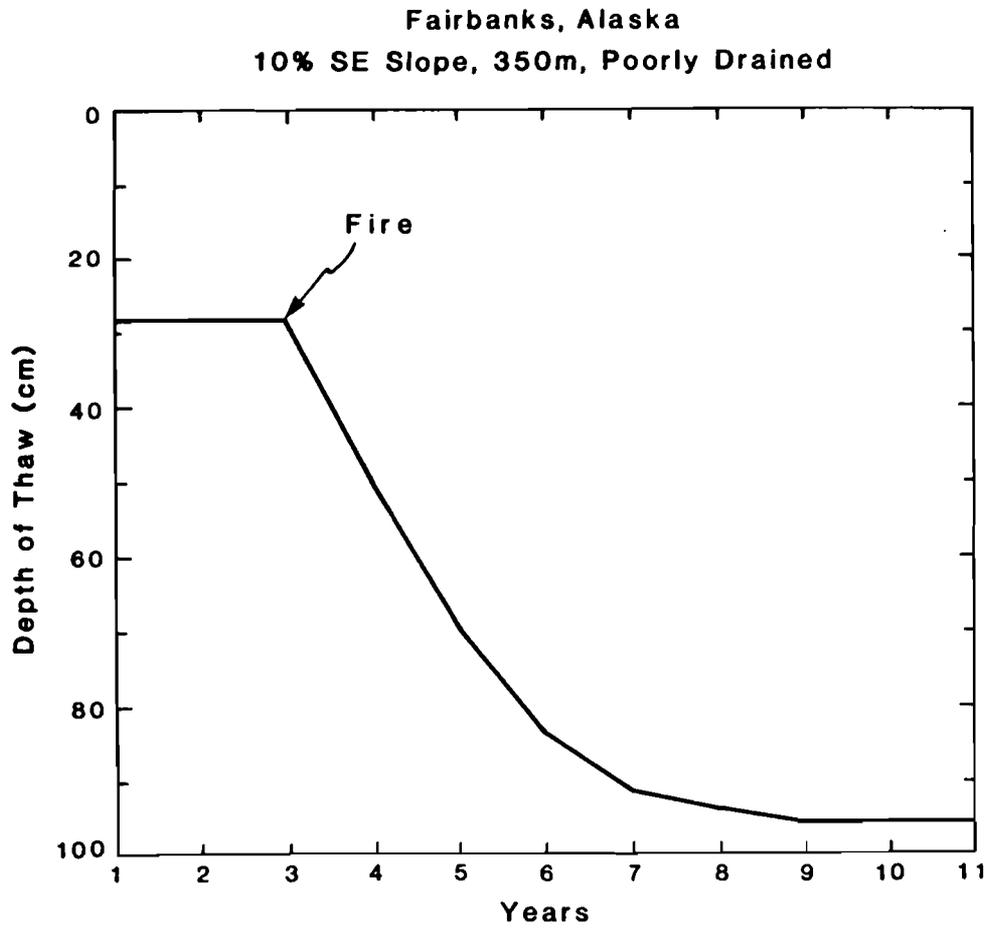
Figure 10. Predicted depth of seasonal thaw in mineral soil at Fairbanks, Alaska, after fire. Pre-burn conditions: moss-organic layer = 25 cm and closed forest canopy. Post-burn conditions: moss-organic layer = 15 cm and open forest canopy.
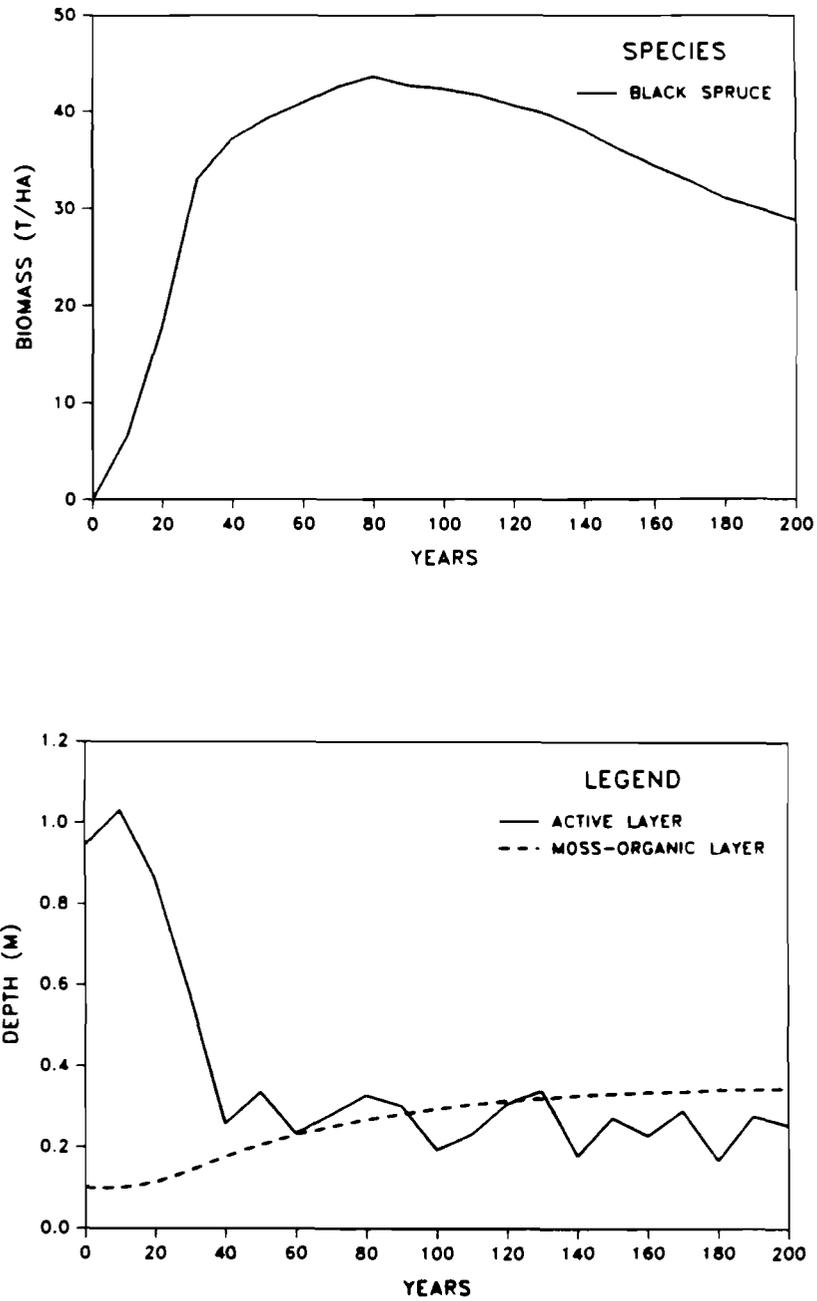
Figure 11. Simulated forest succession and site conditions for 200 years following a catastrophic fire on a poorly-drained, 30% north slope at 350 m elevation, interior Alaska.
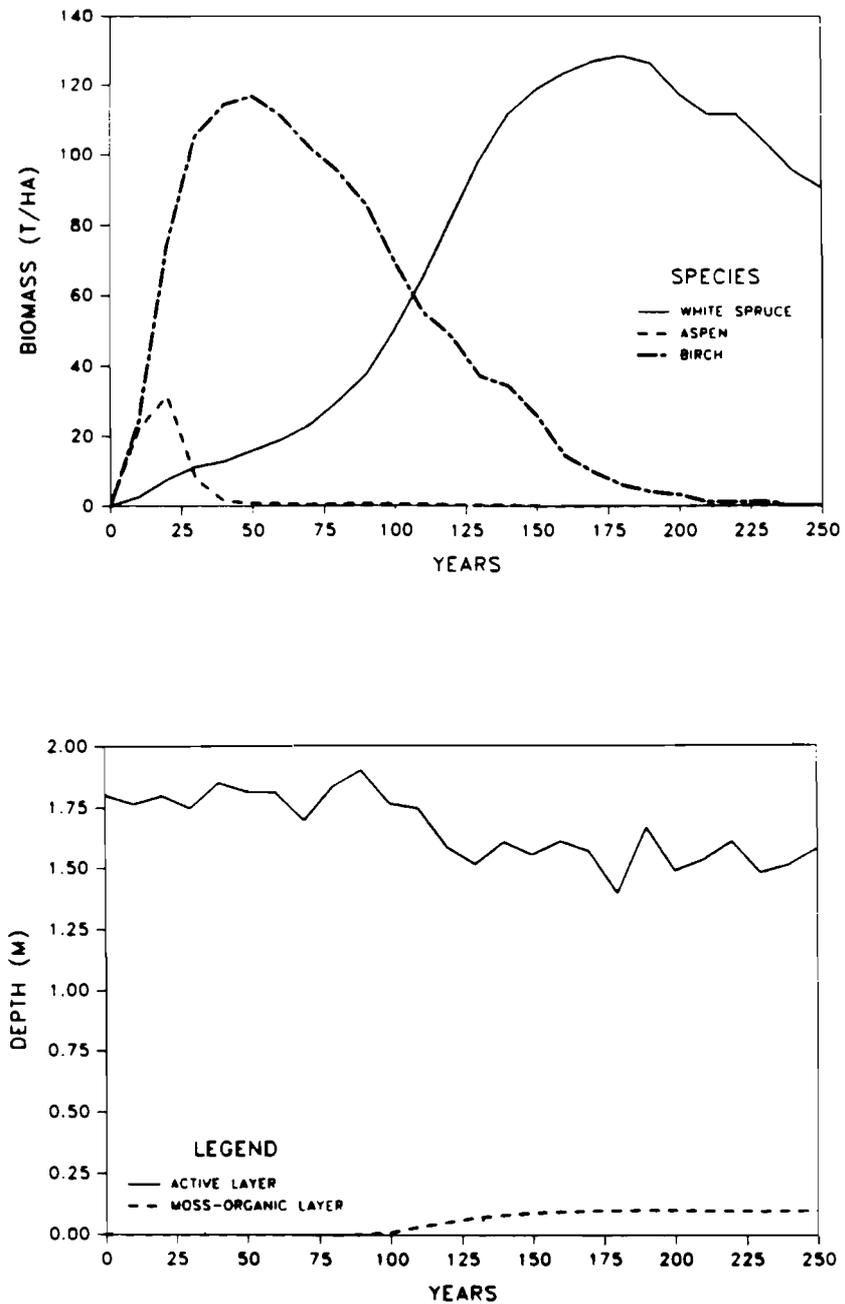
Figure 12. Simulated forest succession and site conditions for 250 years following a catastrophic fire on a well-drained, south slope terrace at 133 m elevation, interior Alaska.
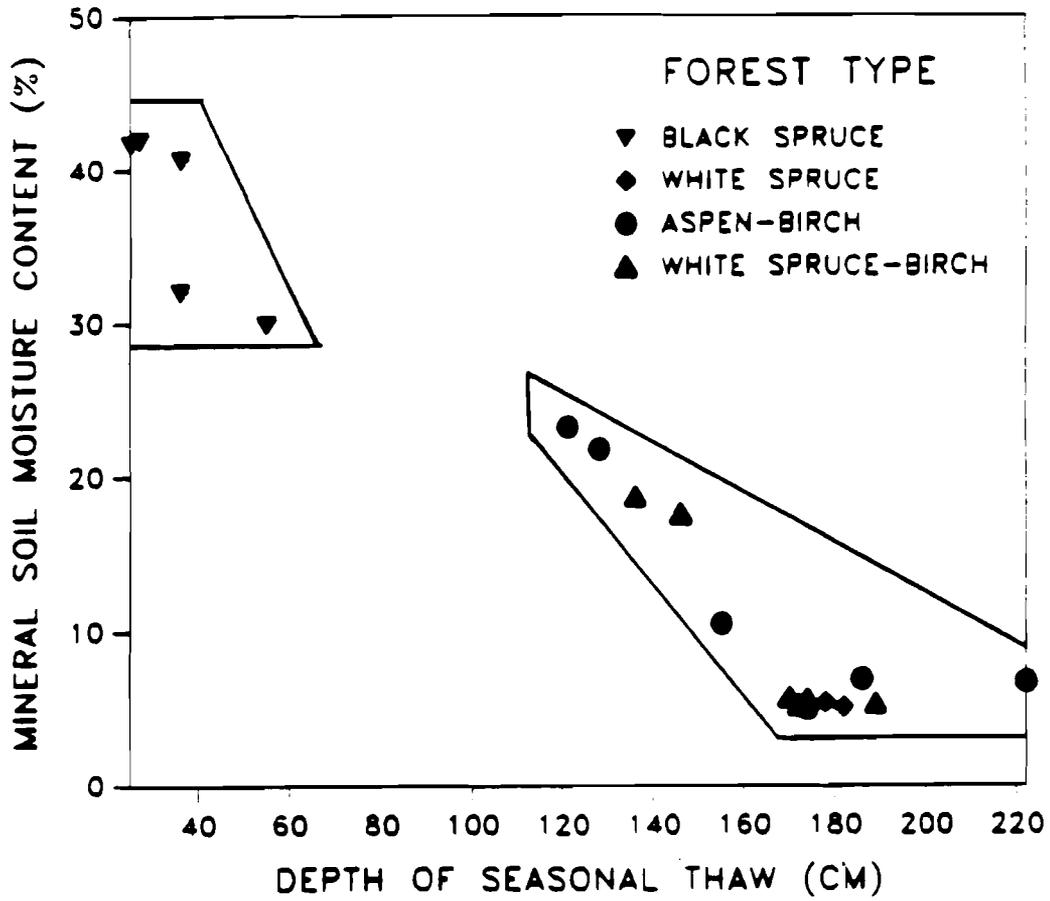
Figure 13. Simulated distribution of upland forest types in relation to depth of thaw and soil moisture.